

ANALYSIS OF RAIN EROSION OF COATED MATERIALS

George S. Springer

Cheng-I. Yang

Poul S. Larsen

Approved for public release;  
distribution unlimited.



## FOREWORD


This report was prepared by the University of Michigan, Department of Mechanical Engineering, Ann Arbor, Michigan, under Air Force Contract F33615-72-C-1563. It was initiated under Project No. 7340, "Nonmetallic and Composite Materials," Task No. 734007 "Coatings for Energy Utilization, Control and Protective Functions." The work was administered under the direction of the Air Force Materials Laboratory, Air Force Systems Command, Wright-Patterson Air Force Base, Ohio, with George F. Schmitt, Jr., of the Elastomers and Coatings Branch, Nonmetallic Materials Division, acting as project engineer.

This report covers the work carried out during the period from June 1972 through May 1973.

The authors wish to thank Mr. G. F. Schmitt, Jr., for his valuable comments and for providing many of the references and data used in this investigation.

This report was submitted by the authors in July 1973.

This technical report has been reviewed and is approved.

  
MERRILL L. MINGES, Acting Chief  
Elastomers and Coatings Branch  
Nonmetallic Materials Division  
Air Force Materials Laboratory

## ABSTRACT

The behavior of coat-substrate systems subjected to repeated impingements of liquid droplets was investigated. The systems studied consisted of a thick homogeneous substrate covered by a single layer of homogeneous coating of arbitrary thickness. Based on the uniaxial stress wave model, the variations of the stresses with time were determined both in the coating and in the substrate. Employing the fatigue theorems established for the rain erosion of homogeneous materials, algebraic equations were derived which describe the incubation period, and the mass loss of the coating past the incubation period, in terms of the properties of the droplet, the coating and the substrate. The results were compared to available experimental data and good agreement was found between the present analytical results and the data.

The differences between the uniaxial stress wave and the uniaxial strain wave models were also evaluated by calculating according to both models a) the stress at the coat-liquid interface, b) the stress that would occur in the substrate in the absence of the coating, and c) the stress in the coating after the first wave reflection from the substrate.

## TABLE OF CONTENTS

Section	Page
I. Introduction	1
II. The Problem	3
III. Stress History of the Coating and the Substrate	9
IV. Incubation Period	20
V. Rate of Mass Removal	31
VI. Total Mass Loss	35
VII. Limits of Applicability of Model	37
VIII. Fatigue Failure of the Substrate	39
IX. Comparison Between the Results of the Uniaxial Stress and Strain Theories	40
X. Summary	47
Appendices	
I. Derivation of Equation 18	52
II. The Value of the Constant $a_1$ for Homogeneous Materials	54
REFERENCES	57

## ILLUSTRATIONS

Figure		Page
1	Droplet Impingement on a Coat-Substrate System. Description of Problem.....	4
2a	Schematic of the Experimental Results.....	7
2b	The Solution Model.....	7
3	Stress Wave Pattern in the Coating and in Substrate.....	10
4	The Variation of the Stress at the Coat-Substrate Interface.....	13
5	The Actual and Approximate Variation of the Stress at the Coat-Substrate Interface.....	15
6	The Variation of the Number of Stress Wave Reflections in the Coating with $\gamma$ .....	17
7	Force Distribution on the Surface of the Coating.....	21
8	The Variation of the Stress with Time at the Liquid Droplet-Coat Interface.....	23
9	Idealized $\sigma_e$ -N Curve.....	26
10	Incubation Period $n_i^*$ versus $S_e/\bar{\sigma}^0$ . Solid Line: Model (Eq. 65). Symbols Defined in Table 1.....	30
11	Rate of Erosion Versus the Inverse of the Incubation Period. Solid Line: Model (Eq. 75). Symbols Defined in Table 1.....	34
12	Comparison of Present Model (Solid Line, Eq. 77b) with Experimental Results. Symbols Defined in Table 1.....	36
13	Rankine-Hugoniot Curve for a Homogeneous Solid.....	41
14	Impact of the Droplet on a Homogeneous Material. Calcu- lation of the Stress at the Liquid-Solid Interface by (a) the Uniaxial Stress Wave Model and (b) the Uniaxial Strain Wave Model.....	43
15	Impact of a Droplet on a Substrate Covered with a Single Layer of Coating. Calculation of the Stress at the Liquid-Coating Interface $\sigma_1$ , the Stress at the Coating- Substrate Interface $\sigma_2$ , and the Stress that Would Occur on the Surface of the Substrate in the Absence of Coating $\sigma_\infty$ . (a) Uniaxial Stress Wave Model; (b) Uniaxial Strain Wave Model.....	45

TABLES

Table		Page
1	Description of Data and Symbols Used in Figures 10, 11 and 12.....	50

## NOMENCLATURE

$a_1$ - $a_6$	constants (dimensionless)
A	area ( $\text{ft}^2$ )
$B_1$ , $B_2$	constant related to wave velocity defined in Eq. (81) (dimensionless)
b	constant defined by Eq. (57) (dimensionless)
$b_1$	constant in Eq. (54) (dimensionless)
$b_2$	knee in the fatigue curve (see Fig. 4)
C	speed of sound (ft/sec)
d	diameter of the droplet (ft)
E	modulus of elasticity ( $\text{lb}/\text{ft}^2$ )
f	number of stress cycles (see Eq. 40)
F	force (lbf)
h	thickness of coat (ft)
I	rain intensity (ft/sec)
$k_e$	number of stress wave reflections in the coating required for the stress at coat-substrate interface to reach a value of 63.3 percent of $\sigma_\infty$ (dimensionless)
$k_L$	total number of stress wave reflections in the coating during the impact period (dimensionless)
$\bar{k}$	average number of stress wave reflections in the coating (dimensionless)
m	mass eroded per unit area ( $\text{lb}/\text{ft}^2$ )
$m^*$	dimensionless mass loss defined by Eq. (76)
n	number of drops impinging per unit area ( $\text{number}/\text{ft}^2$ )
$n^*$	number of drops impinging per site, see Eq. (61) (dimensionless)
$n_a^*$	characteristic life (dimensionless)
N	fatigue life (see Fig. 4) (dimensionless)



P	probability defined by Eq. (27) (dimensionless)
P	stress (lbf/ft <sup>2</sup> )
q	drop density (number/ft <sup>3</sup> )
r	distance (ft)
S	parameter defined by Eq. (59) (lbf/ft <sup>2</sup> )
S <sub>e</sub>	parameter defined by Eq. (60) (lbf/ft <sup>2</sup> )
t	time (sec)
t <sub>e</sub>	time required for k <sub>e</sub> number of stress wave reflections to take place in the coating (sec)
t <sub>L</sub>	the duration of impact (sec)
u	particle velocity (ft/sec)
v	wave velocity defined by Eq. (81)
V	velocity of impact (ft/sec)
V <sub>t</sub>	terminal velocity of a rain droplet (ft/sec)
W	weight loss due to erosion (lbf)
Z	dynamic impedance (lbm/(ft <sup>2</sup> -sec))

#### GREEK LETTERS

α	rate of mass loss (lbm/impact) (see Fig. 2b)
α*	dimensionless rate of mass loss (see Eq. 73)
β	Weibull slope in Eq. (67) (dimensionless)
γ	the ratio of k <sub>L</sub> to k <sub>e</sub> (γ=k <sub>L</sub> /k <sub>e</sub> )
ν	Poisson's ratio (dimensionless)
ρ	density (lbm/ft <sup>3</sup> )
θ	angle (radians)
σ	stress (lbf/ft <sup>2</sup> )
σ <sub>a</sub>	stress amplitude (lbf/ft <sup>2</sup> )

$\sigma_e$	equivalent dynamic stress defined by Eq. (42) (lbf/ft <sup>2</sup> )
$\sigma_m$	mean stress (lbf/ft <sup>2</sup> )
$\bar{\sigma}$	mean stress after $k_L$ number of stress wave reflections (lbf/ft <sup>2</sup> )
$\sigma_I$	endurance limit (lbf/ft <sup>2</sup> )
$\sigma_u$	ultimate tensile strength (lbf/ft <sup>2</sup> )
$\psi$	parameter defined by Eqs. (13)-(14)

#### SUBSCRIPTS

c	coating
i	end of incubation period
f	upper limit of validity of model
k	the number of stress wave reflections in the coating
L	liquid
s	solid
sc	coat-substrate interface
Lc	liquid-coat interface

#### SUPERSCRIPTS

B	uniaxial strain wave model
h	coat-substrate interface
o	liquid-coat interface

## SECTION I

### INTRODUCTION

Components of high speed aircraft and missiles may experience heavy damage when subjected to repeated impingements of rain droplets. The damage to nonmetallic components, such as plastic radomes, may be particularly severe. To protect such surfaces from rain erosion, these surfaces are frequently covered with a thin layer of coating. Considerable research has been performed in the past to select the most suitable coating material, and to determine the behavior of various coat-substrate systems undergoing liquid impingement.

The majority of the previous studies of rain erosion of coated materials have been experimental in nature, with the bulk of prior research concentrating on the measurement of an erosion parameter (e.g. weight loss) under specific conditions (References 1-6). These experimental studies provide information on the behavior of a given coat-substrate combination under a given condition, but fail to describe material behavior beyond the range of the experiments in which they were obtained. For the selection of the proper materials and for the design of the appropriate structures an analytical or semiempirical model would be needed, which would describe the response of coat-substrate systems in terms of the relevant parameters. These parameters should include the properties of the coating and the substrate, the thickness of the coating, and the impact velocity and size of the droplet. In recent years, progress towards this goal has been made by Morris (Reference 7), Engel and Piekutowski (Reference 8) and by Conn and his coworkers (References 9-11), who analyzed the stress history in various coat-substrate systems. Al-

though the results of these investigations further our understanding of the processes which contribute to the failure of the coating and the substrate, as yet they are not capable of correlating fully the existing data and generalizing the results obtained from a few experiments.

The objective of this investigation is to develop a model which is consistent with experimental observation and which predicts quantitatively "erosion" of coated materials under previously untested conditions. In particular, the model proposed here is aimed at describing a) the "incubation period", i.e. the time elapsed before the mass loss of the coating becomes appreciable, and b) the degradation of the coating past the incubation period, as manifested by its mass loss. The model is based on fatigue concepts (e.g. References 12, 13), and is along the lines developed previously for homogeneous (uncoated) materials (Reference 13). The success of this model in describing the damage of homogeneous materials warranted its extension to coated materials.

## SECTION II

### THE PROBLEM

The problem investigated is the following. Spherical liquid droplets impinge repeatedly upon a plane, semi-infinite material consisting of a homogeneous substrate covered by a homogeneous coating (Fig. 1). The thickness of the coating is  $h$ . The substrate is taken to be semi-infinite normal to the plane of the surface ( $x$  direction in Fig. 1). The coating and the substrate are characterized by the following properties: density  $\rho$ , speed of sound  $C$ , modulus of elasticity  $E$ , Poisson's ratio  $\nu$ , ultimate tensile strength  $\sigma_u$  and endurance limit  $\sigma_I$ . Parameters related to the coating and the substrate are denoted by  $c$  and  $s$ , respectively. Parameters related to the droplet are identified by the subscript  $L$ .

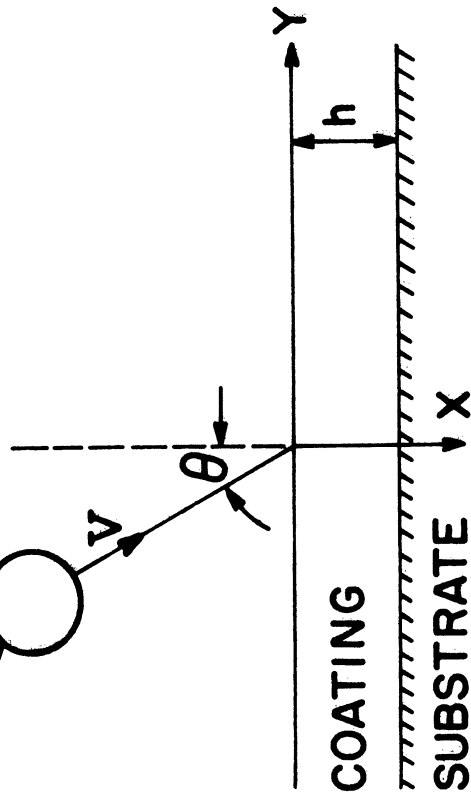
A perfect bond is assumed between the coating and the substrate, i.e. at the interface ( $x=h$ ) the stresses and the displacements are the same in the coating and the substrate. Furthermore, the stress wave propagating through the coating and the substrate are considered to be one dimensional, propagating normal to the surface (compression waves). Waves parallel to the surface (shear waves) are neglected.

The diameter of the droplets  $d$ , the angle of incidence  $\theta$ , and the velocity of impact  $V$  are taken to be constant. The spatial distribution of the droplets is considered to be uniform. Accordingly, the number of droplets impinging on unit area in time  $t$  is (Reference 13)

$$n = (V \cos \theta) q t \quad (1)$$

where  $q$  is the number of droplets per unit volume. Rain, falling with constant terminal velocity  $V_t$ , is usually characterized by a parameter  $I$

**DROPLET**  
 Diameter:  $d$   
 Density:  $\rho_L$   
 Speed of Sound:  $C_L$



Density:	$\rho_C$	$\rho_S$
Speed of Sound:	$C_C$	$C_S$
Modulus of Elasticity:	$E_C$	$E_S$
Poisson Ratio:	$\nu_C$	$\nu_S$
Ultimate Tensile Strength:	$(\sigma_U)_C$	$(\sigma_U)_S$
Endurance Limit:	$(\sigma_I)_C$	$(\sigma_I)_S$
Thickness:	$h$	Semi-infinite

Fig. 1. Droplet Impingement on a Coat-Substrate System. Description of Problem.

called "intensity" (with units of length/time) which is related to  $q$  by the expression

$$q = \frac{6}{\pi} \frac{I}{V_t d^3} \quad (2)$$

Equations (1) and (2) may be combined to yield

$$\dot{n} = \frac{6}{\pi} \frac{(V \cos \theta) I}{V_t d^3} t \quad (3)$$

The impingement rate is assumed to be sufficiently low so that all the effects produced by the impact of one droplet diminish before the impact of the next droplet (References 13, 14).

The pressure within the droplet varies both with position and with time. For simplicity, the pressure at the liquid-surface interface is taken to be constant, its value being given by the water hammer pressure (Reference 15)

$$P = \frac{\rho_L C_L V \cos \theta}{1 + \frac{\rho_L C_L}{\rho_c C_c}} \quad (4)$$

Although more accurate representation of the pressure is possible (Reference 15) the accuracies afforded by the use of equation (4) will suffice in the present analysis. The duration of the pressure at the interface is approximated by

$$t_L = \frac{2d}{C_L} \quad (5)$$

The forces, created by the repeated droplet impacts, damage the material as manifested by the formation of pits and cracks on the surface, and by weight loss of the coating material. Experimental evidence indicates that under a wide range of conditions the weight loss  $W$  varies with time  $t$

as shown, schematically, in Fig. 2a. For some period of time, referred to as incubation period, the weight loss is insignificant. Between the end of the incubation period  $t_i$  and a time denoted by  $t_f$  the weight loss varies nearly linearly with time. After  $t_f$  the relationship between  $W$  and  $t$  becomes more complex. Here, we will be concerned only with the behavior of the material up to time  $t_f$ . In most practical situations the usefulness of the material does not extend beyond  $t_f$ .

It is advantageous to replace the total weight loss of the sample by the mass loss per unit area  $m$ , and the time by the number of droplets impinging upon unit area  $n$ . In terms of the parameters  $m$  and  $n$ , schematic representation of the data is given in Fig. 2b. It is now assumed that the data can be approximated by two straight lines as shown in Fig. 2b, i.e.

$$m = 0 \qquad 0 < n < n_i \qquad (6a)$$

$$m = \alpha (n - n_i) \qquad n_i < n < n_f \qquad (6b)$$

Thus, the material loss  $m$  produced by a certain number of impacts  $n$ , can be calculated once the incubation period  $n_i$  and the rate of subsequent mass loss (as characterized by the slope  $\alpha$ ) are known. Therefore, the problem at hand is to determine the parameters  $n_i$ ,  $\alpha$ , and  $n_f$ , the latter being the upper limit of validity of equation (6b). It is noted here that the above model is valid only if there is an incubation period. Problems in which even one impact results in appreciable damage will not be considered.



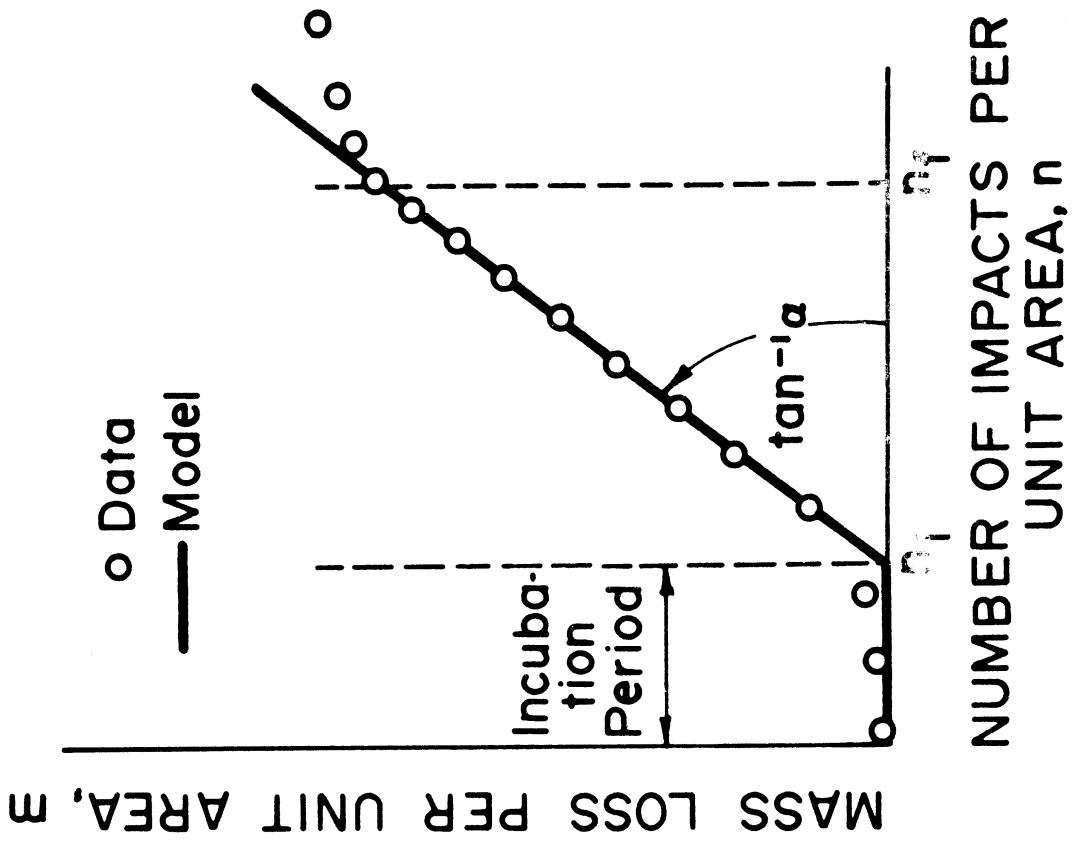


Fig. 2b. The Solution Model

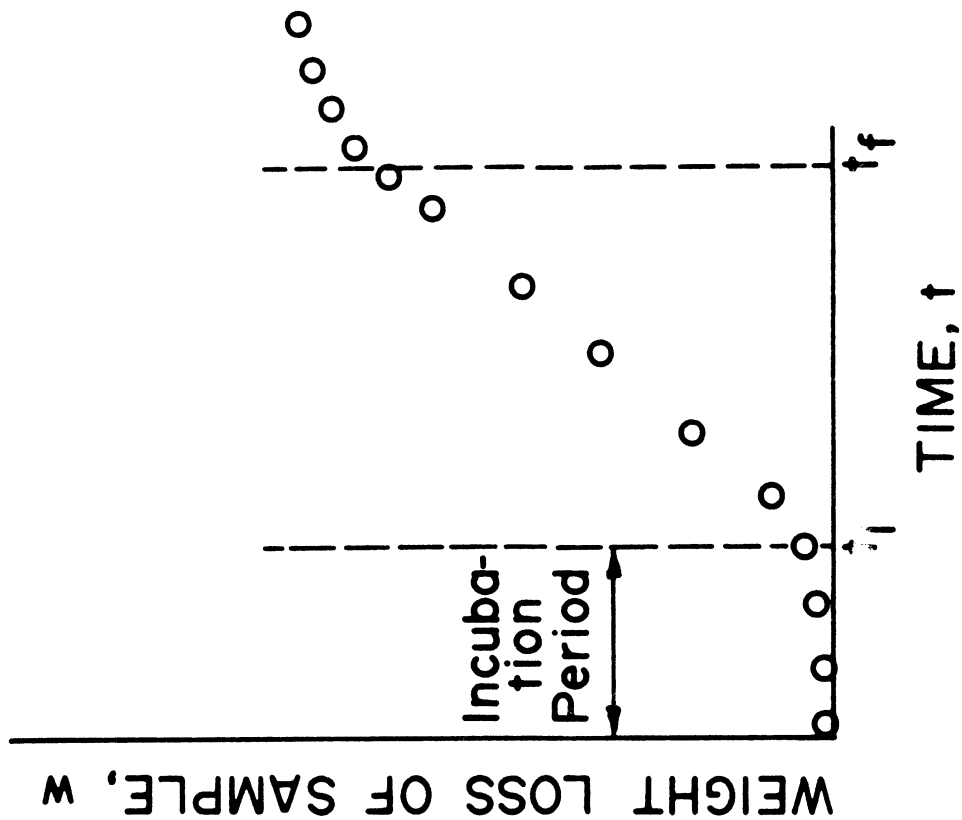


Fig. 2a. Schematic of the Experimental Results

In order to establish  $n_1$  and  $\alpha$ , the stress history in the coating must be known. Thus, first expressions are derived which describe, in suitable form, the variation of the stress with time in the coating and in the substrate.

### SECTION III

#### STRESS HISTORY OF THE COATING AND THE SUBSTRATE

The variation of the stress with time may be evaluated by considering either uniaxial stress waves (References 10, 11) or uniaxial strain waves (References 6, 7) propagating through the coating. As will be shown in Section VIII these two approaches yield similar results. The present calculations are based on the uniaxial stress wave model.

When a liquid droplet impinges upon the surface of the coating, a stress wave propagates through the coating (see Fig. 3). The magnitude of this initial stress wave, denoted by  $\sigma_1$ , is identical to the hydrostatic pressure  $P$ , i.e.,

$$\sigma_1 = P \quad (7)$$

$P$  is given by equation (4). At the coat-substrate interface a portion of the stress wave is transmitted into the substrate while a portion of it is reflected back into the coating. Thus, there is a "left" traveling wave in the coating of magnitude  $\sigma_2$  (Fig. 3)

$$\sigma_2 = \sigma_1 + \sigma_r^h \quad (8)$$

In equation (8)  $\sigma_r^h$  represents the magnitude of the reflected wave which may be expressed as (Reference 8)

$$\sigma_r^h = \sigma_1 \frac{Z_s - Z_c}{Z_s + Z_c} \quad (9)$$

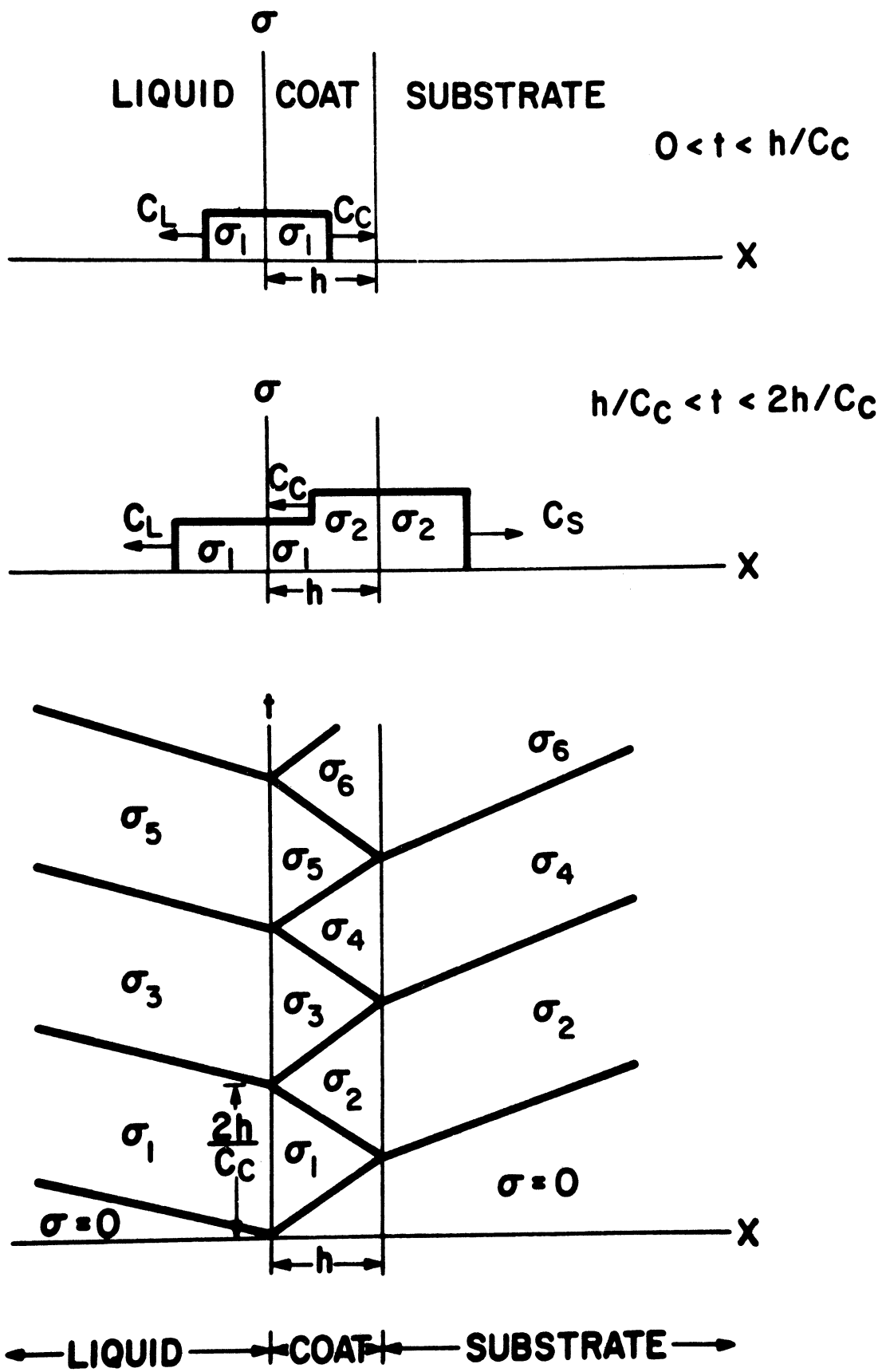


Fig. 3. Stress Wave Pattern in the Coating and in Substrate.

In the time interval  $t=C/2h$  the "left" traveling  $\sigma_2$  wave reaches the coat-liquid interface and a new "right" traveling wave of magnitude  $\sigma_3$  is generated at the  $x=0$  surface

$$\sigma_3 = \sigma_2 + \sigma_r^0 \quad (10)$$

where  $\sigma_r^0$  is the reflected wave from the surface of the coating (Reference 8)

$$\sigma_r^0 = \sigma_2 \frac{Z_L - Z_c}{Z_L + Z_c} \quad (11)$$

In equations (9) and (11)  $Z$  is the impedance of the material

$$Z \equiv \rho C \quad (12)$$

Introducing the notation

$$\psi_{sc} \equiv \frac{Z_s - Z_c}{Z_s + Z_c} \quad (13)$$

$$\psi_{Lc} \equiv \frac{Z_L - Z_c}{Z_L + Z_c} \quad (14)$$

the magnitudes of the "left" and "right" traveling waves become

$$\begin{aligned} \sigma_1 &= P \\ \sigma_2 &= \sigma_1 + \sigma_1 \psi_{sc} = \sigma_1 (1 + \psi_{sc}) \\ \sigma_3 &= \sigma_1 (1 + \psi_{sc} + \psi_{sc} \psi_{Lc}) \\ \sigma_4 &= \sigma_1 (1 + \psi_{sc} + \psi_{sc} \psi_{Lc} + \psi_{sc} \psi_{Lc} \psi_{sc}) \end{aligned} \quad (15)$$

etc.

Equations (15) may readily be generalized to the following forms

$$\frac{\sigma_{2k}}{\sigma_1} = \frac{1 + \psi_{sc}}{1 - \psi_{sc}\psi_{Lc}} [1 - (\psi_{sc}\psi_{Lc})^k] \quad (16)$$

$$\frac{\sigma_{2k-1}}{\sigma_1} = \frac{\sigma_{2k}}{\sigma_1} - \psi_{sc}(\psi_{sc}\psi_{Lc})^{k-1} \quad (17)$$

where  $k$  is an integer,  $k = 1, 2, 3, \dots$

Note that the stress history in the coating depends on the relative magnitudes of  $Z_L$ ,  $Z_c$  and  $Z_s$ . This is illustrated in Fig. 4, where the variation of the stress with time is shown for the four possible combinations of impedances. After a long period of time (i.e. after a large number of reflections,  $k \rightarrow \infty$ ) the stress at both on the surface of the coating ( $x=0$ ) and at the coat-substrate interface ( $x=h$ ) approaches the constant value

$$\sigma_\infty = \sigma_1 \lim_{k \rightarrow \infty} \frac{\sigma_{2k}}{\sigma_1} = \frac{1 + \psi_{sc}}{1 - \psi_{sc}\psi_{Lc}} = \frac{1 + Z_L/Z_c}{1 + Z_L/Z_s} \quad (18)$$

$\sigma_\infty$  is the stress that would occur in the substrate if the droplet would impinge upon it directly in the absence of a coating (see Appendix I). It is evident from Fig. 4 that the coating reduces the stresses in the substrate only if the appropriate coating material (i.e. appropriate combination of  $Z_L$ ,  $Z_c$  and  $Z_s$ ) is selected (Figs. 4c and 4d). For certain combinations of coating and substrate the mean stresses in the substrate are actually higher with the coating than without it (Figs. 4a and 4b). This result clearly indicates the importance of the proper selection of the material used as coating for a particular substrate.

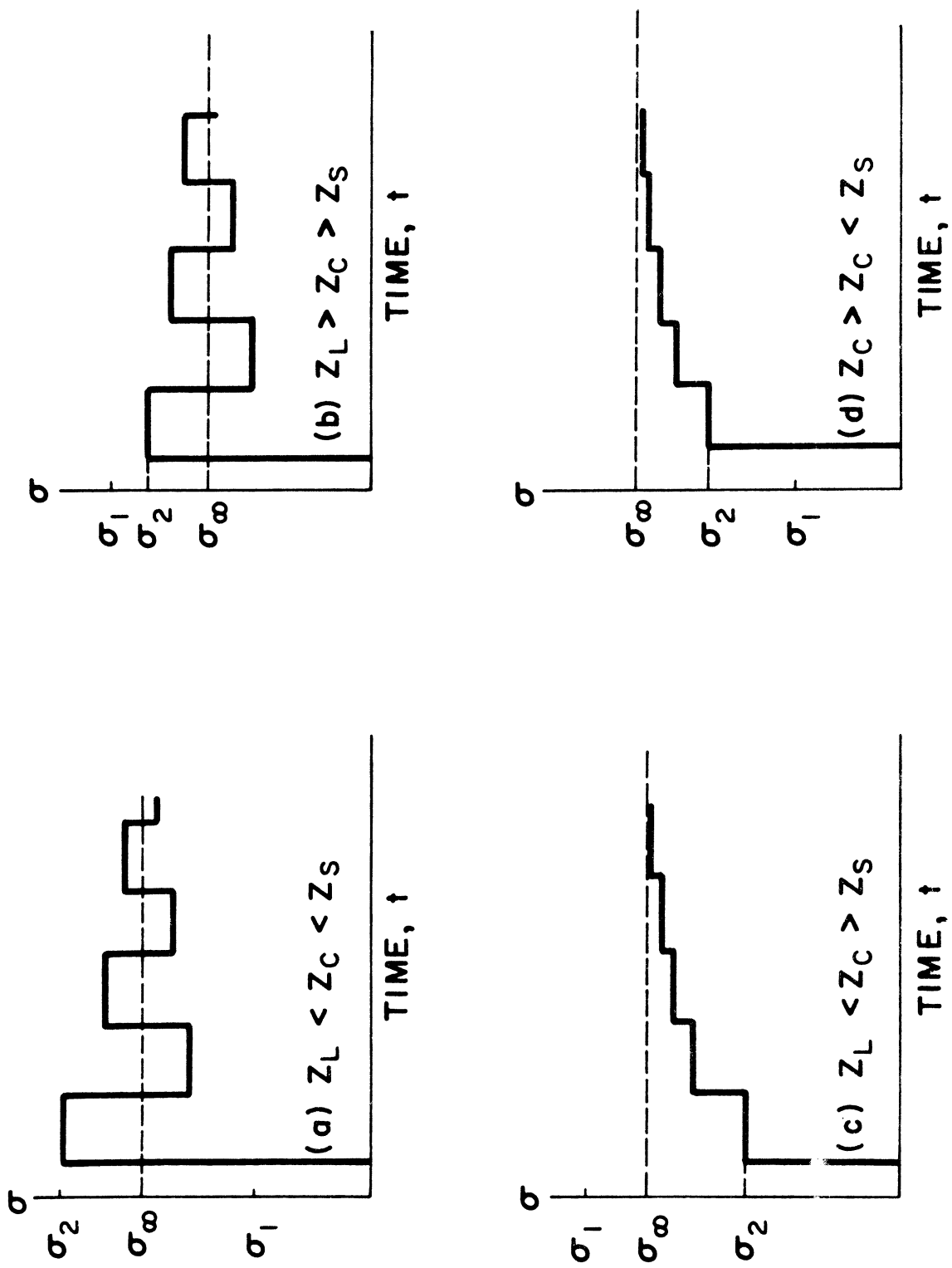


Fig. 11. The Variation of the Stress at the Coat-Substrate Interface.

Equations (16) and (17) describe the variation of the stress with time in the coating. For our further calculations it is convenient to replace the stepwise variation of the stress by a continuous function. To accomplish this, equation (16) is rewritten in the form

$$\frac{\sigma_{2k}}{\sigma_1} = \frac{\sigma_\infty}{\sigma_1} - \left( \frac{\sigma_\infty}{\sigma_1} - \frac{\sigma_2}{\sigma_1} \right) (\psi_{sc} \psi_{Lc})^{k-1} \quad (19)$$

Equation (19) is now approximated by the expression

$$\frac{\sigma_{2k}}{\sigma_1} = \frac{\sigma_\infty}{\sigma_1} - \left( \frac{\sigma_\infty}{\sigma_1} - \frac{\sigma_2}{\sigma_1} \right) \exp \left( - \frac{k-1}{k_e} \right) \quad (20)$$

By replacing equation (19) by equation (20) we replace, in effect, the stepwise stress function with an exponential curve, as illustrated in Fig. 5. In equation (20)  $k_e$  is the number of reflections required for the stress to reach 63.3 percent of  $\sigma_\infty$ . To evaluate  $k_e$  we introduce the condition that the area under the actual (stepwise) and the exponential curves are to be the same. This condition requires that the following equality be satisfied

$$\sum_{k=1}^{\infty} \left[ \frac{\sigma_\infty}{\sigma_1} - \left( \frac{\sigma_\infty}{\sigma_1} - \frac{\sigma_2}{\sigma_1} \right) (\psi_{sc} \psi_{Lc})^{k-1} \right] = \int_1^{\infty} \left[ \frac{\sigma_\infty}{\sigma_1} - \left( \frac{\sigma_\infty}{\sigma_1} - \frac{\sigma_2}{\sigma_1} \right) \exp \left( - \frac{k-1}{k_e} \right) \right] dk \quad (21)$$

Evaluating the summation and the integral in equation (21) we obtain

$$k_e = \frac{1}{1 - \psi_{sc} \psi_{Lc}} \quad (22)$$

Substitution of equations (13) and (14) into equation (22) yields

$$k_e = \frac{1 + Z_L/Z_s}{2} \frac{1 + Z_c/Z_s}{1 + Z_L/Z_s} \quad (23)$$

In the absence of coating  $Z_s = Z_c$  and  $k_e = 1$ , which, as expected, shows that there are no reflections in a semi-infinite material.



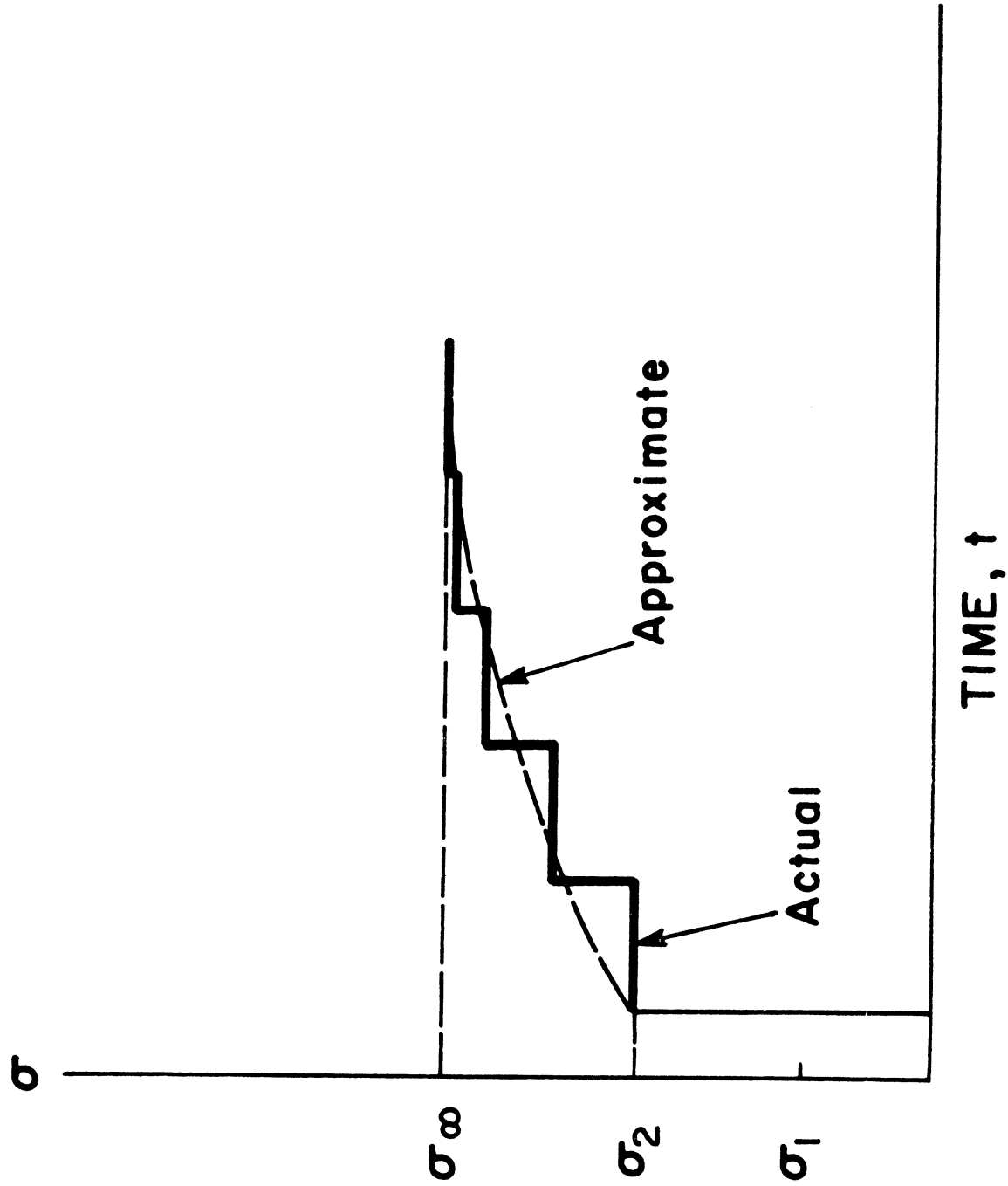


Fig. 5. The Actual and Approximate Variation of the Stress at the Coat-Substrate Interface.

The time required for  $k_e$  number of reflections to occur is (see Fig. 3)

$$t_e = k_e \frac{2h}{C_c} \quad (24)$$

and the number of reflections during this time is

$$k_e = t_e \frac{C_c}{2h} \quad (25)$$

Similarly, the number of reflections which occur during the duration of the impact  $t_L$  (given by equation 5) is

$$k_L = t_L \frac{C_c}{2h} = \frac{C_c}{C_L} \frac{d}{h} \quad (26)$$

It is to be noted that  $k_e$  is independent of the thickness of the coating (see equation 23), while  $k_L$  depends on  $h$ . For thick coating ( $h/d \rightarrow \infty$ )  $k_L \rightarrow 0$  and for thin coating ( $h/d \rightarrow 0$ )  $k_L \rightarrow \infty$ . Thus, the ratio

$$\gamma = \frac{k_L}{k_e} \quad (27)$$

may vary between zero and infinity. It is convenient to bridge these two limits by the exponential curve

$$\bar{k} = k_e [1 - \exp(-\frac{k_L}{k_e})] \quad (28)$$

or

$$\bar{k} = k_e [1 - \exp(-\gamma)] \quad (29)$$

$\bar{k}$  represents the average number of reflections in the coating. The variation of  $\bar{k}$  with  $\gamma$  is illustrated in Fig. 6. For thick coating  $\bar{k}$  becomes

$$\bar{k}_{h/d \rightarrow \infty} = 0 \quad (30)$$

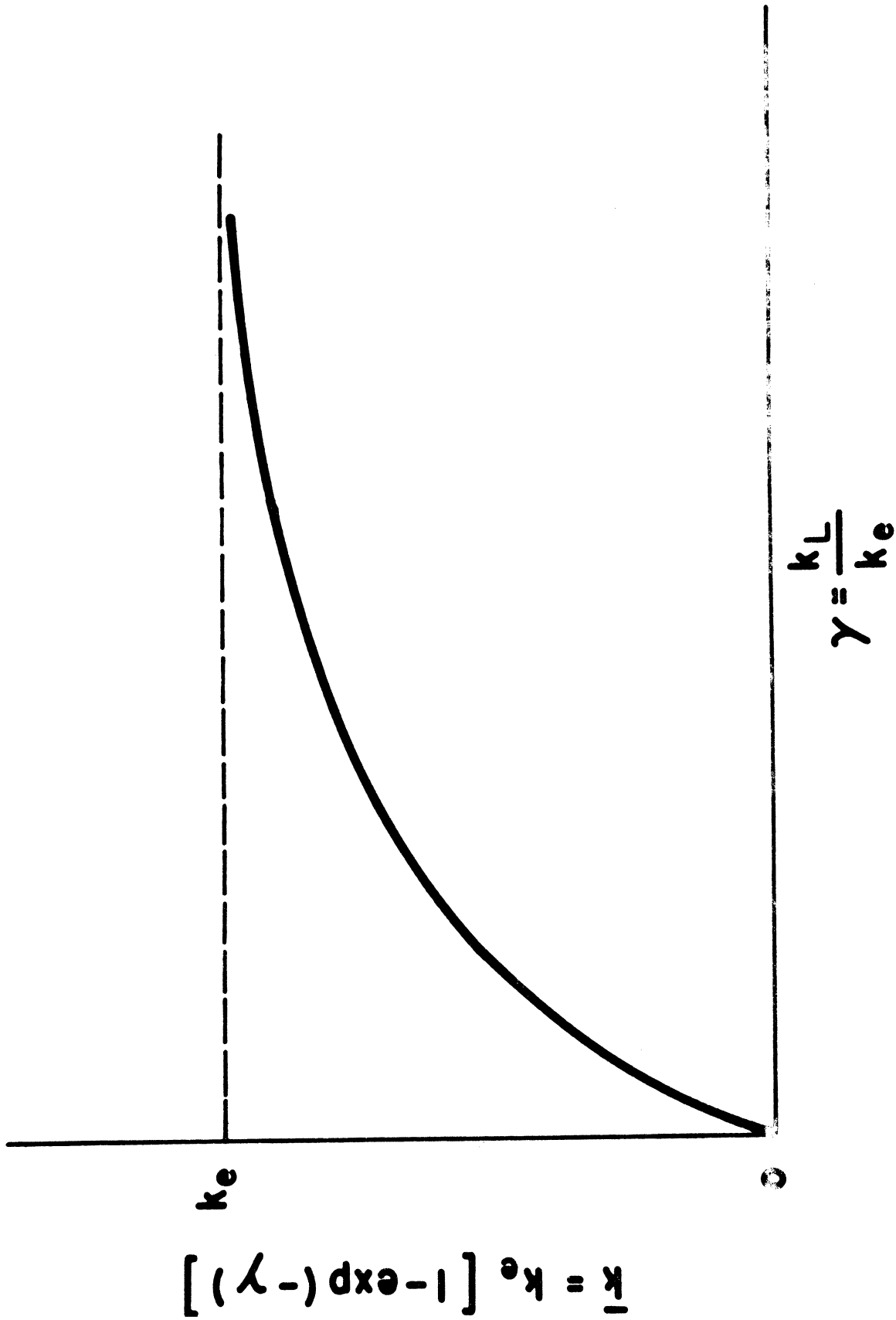


Fig. 6. The Variation of the Number of Stress Wave Reflections in the Coating with  $\gamma$ .

For thin coating equation (29) reduces to

$$k_{h/d} \rightarrow 0 = k_e \quad (31)$$

which is, by our definition, the maximum number of reflections which may occur in the coating.

We may evaluate now the average values of the stresses at the coat-liquid ( $x=0$ ) and at the coat-substrate interfaces ( $x=h$ ) during the period of impact  $t_L$ . The average stress at  $x=0$  is

$$\bar{\sigma}^0 = \frac{1}{k_L} \sum_{k=1}^{k_L} \sigma_{2k-1} \quad (32)$$

and at  $x=h$  is

$$\bar{\sigma}^h = \frac{1}{k_L} \sum_{k=1}^{k_L} \sigma_{2k} \quad (33)$$

Substituting equations (16), (17) and (18) into equations (32) and (33) and utilizing the exponential approximation given by equation (20), after some algebraic manipulation, we obtain

$$\frac{\bar{\sigma}^0}{\sigma_1} = \frac{1 + \psi_{sc}}{1 - \psi_{sc}\psi_{Lc}} \left[ 1 - \psi_{sc} \frac{1 + \psi_{Lc}}{1 + \psi_{sc}} \frac{1 - \exp(-\gamma)}{\gamma} \right] \quad (34a)$$

$$\frac{\bar{\sigma}^h}{\sigma_1} = \frac{1 + \psi_{sc}}{1 - \psi_{sc}\psi_{Lc}} \left[ 1 - \psi_{sc}\psi_{Lc} \frac{1 - \exp(-\gamma)}{\gamma} \right] \quad (34b)$$

If the coating is of the same material as the substrate  $\psi_{sc}=0$  and equation (34a) reduces to

$$\bar{\sigma}^0 = \sigma_1 = P \quad (35)$$

The force exerted by the droplet on the surface of the coating also varies with time. The average force on the surface during the duration of one impact  $t_L$  is

$$\bar{F} = \bar{\sigma}^0 \frac{\pi d^2}{4} \quad (36)$$

The foregoing equations describe the stress history in the coating and in the substrate when the substrate is covered by a single layer of coating. The results could be generalized readily to include two or more layers of coatings. It is emphasized, however, that the expressions here developed are not restricted to thin coatings, but may be applied to coatings of arbitrary thicknesses. The thickness of the coating enters the results through the parameter  $\gamma$ . From equations (23), (26) and (27) we have

$$\gamma = \frac{C_c}{C_L} \frac{d}{h} \left( \frac{1 + Z_L/Z_s}{1 + Z_c/Z_s} \right) \left( \frac{1 + Z_L/Z_s}{2} \right) \quad (37)$$

For a thick coating ( $h/d \rightarrow \infty$ )  $\gamma$  becomes

$$\gamma_{h/d \rightarrow \infty} = 0 \quad (38)$$

For a thin coating ( $h/d \rightarrow 0$ )  $\gamma$  assumes the value

$$\gamma_{h/d \rightarrow 0} = \infty \quad (39)$$

SECTION IV  
INCUBATION PERIOD

It has been recognized in the past that fatigue plays an important role in the erosion process (References 12, 14, 16-21), particularly in the "early" stages of the process, corresponding to the incubation period. Applying fatigue concepts to the problem of rain erosion, Springer and Baxi (Reference 13) recently established a semiempirical formula which describes the incubation period in a homogeneous material. Here, Springer and Baxi's analysis is extended to homogeneous materials covered by a single layer of coating. The analysis is based on the concept that fatigue theorems established for the torsion and bending of bars might be applied, at least qualitatively, to materials subjected to repeated liquid impingement. The failures of bars undergoing repeated torsion or bending have been found to follow Miner's rule (Reference 22)

$$\frac{f_1}{N_1} + \frac{f_2}{N_2} + \dots + \frac{f_q}{N_q} = a_1 \quad (40)$$

where  $f_1, f_2 \dots f_q$  represent the number of cycles the specimen is subjected to specified overstress levels  $\sigma_{e1}, \sigma_{e2} \dots \sigma_{eq}$ , and  $N_1, N_2, \dots, N_q$  represent the life (in cycles) at these overstress levels, as given by the fatigue ( $\sigma_e$  versus  $N$ ) curve.  $a_1$  is a constant.

Let us now consider a point B on the surface of the material as shown in Fig. 7. Each droplet impinging upon the surface creates a stress at point B. Assuming that the force created by the droplet at its point of impact is a "point force", the stress at point B due to any one

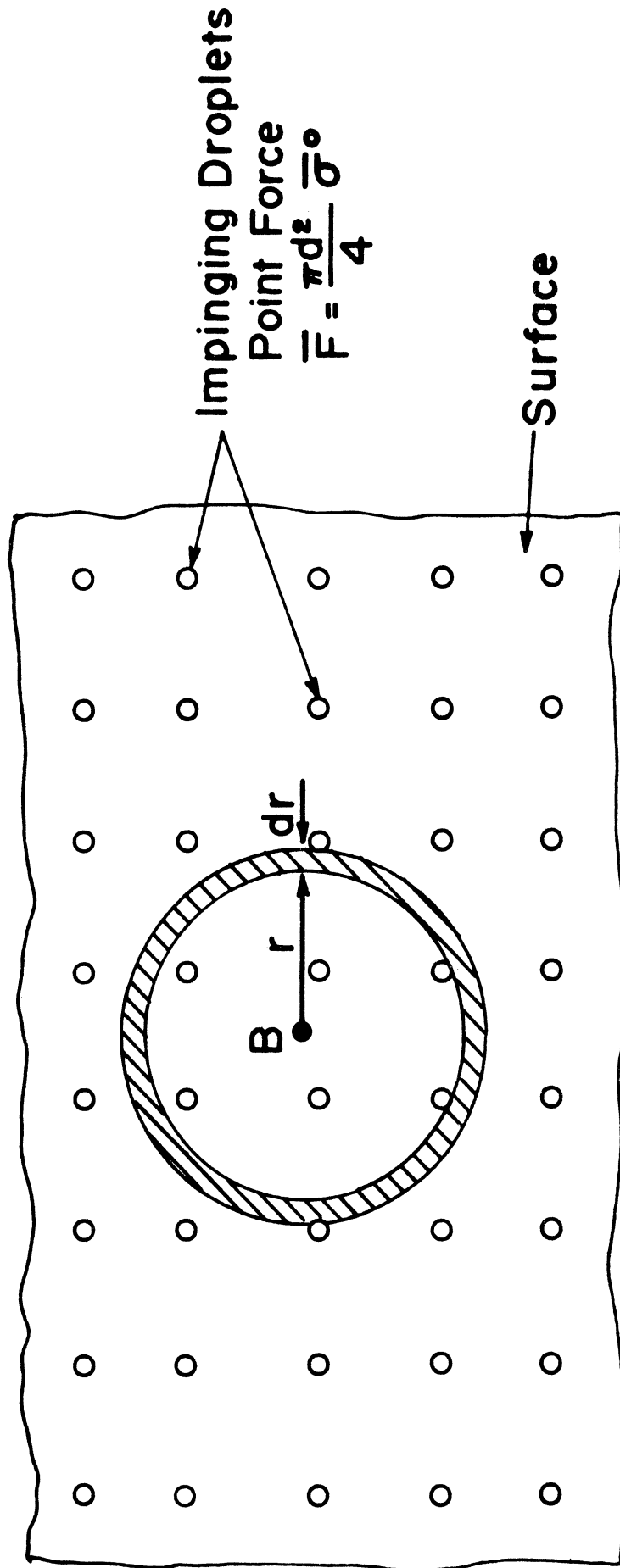


Fig. 7. Force Distribution on the Surface of the Coating.

droplet is (Reference 23)

$$\sigma = \frac{\bar{P} (1-\nu_c)}{2\pi r^2} \quad (41)$$

where  $\bar{P}$  is given by equation (36). Due to the propagation and reflection of the stress waves in the coating (as discussed in the previous section) the stress in the coating does not remain constant, but fluctuates, as illustrated in Fig. 8. Fatigue life of the material is generally calculated using an "equivalent dynamic stress" (Reference 24)

$$\sigma_e = \frac{\sigma_a \sigma_m}{\sigma_u - \sigma_m} \quad (42)$$

where  $\sigma_u$  is the ultimate tensile strength of the material. In the present case  $\sigma_e$  may be separated into two parts  $\sigma_e = \sigma'_e + \sigma''_e$ . The first part,  $\sigma'_e$  is due to oscillations about the mean  $\sigma'_m = \sigma$  with amplitude  $\sigma'_a$ . The second part  $\sigma''_e$  is due to "oscillation" about the mean  $\sigma''_m = \sigma/2$ , with a constant amplitude  $\sigma''_a = \sigma/2$ . Thus,  $\sigma'_a$  is not a constant but varies with time. For simplicity, we assume that  $\sigma'_a$  is a constant with a value equivalent to the maximum amplitude, i.e.

$$\sigma'_a \approx |\sigma_2 - \sigma| \quad (43)$$

Equations (36) and (43) yield

$$\sigma'_a \approx \sigma |\psi_{sc}| \quad (44)$$



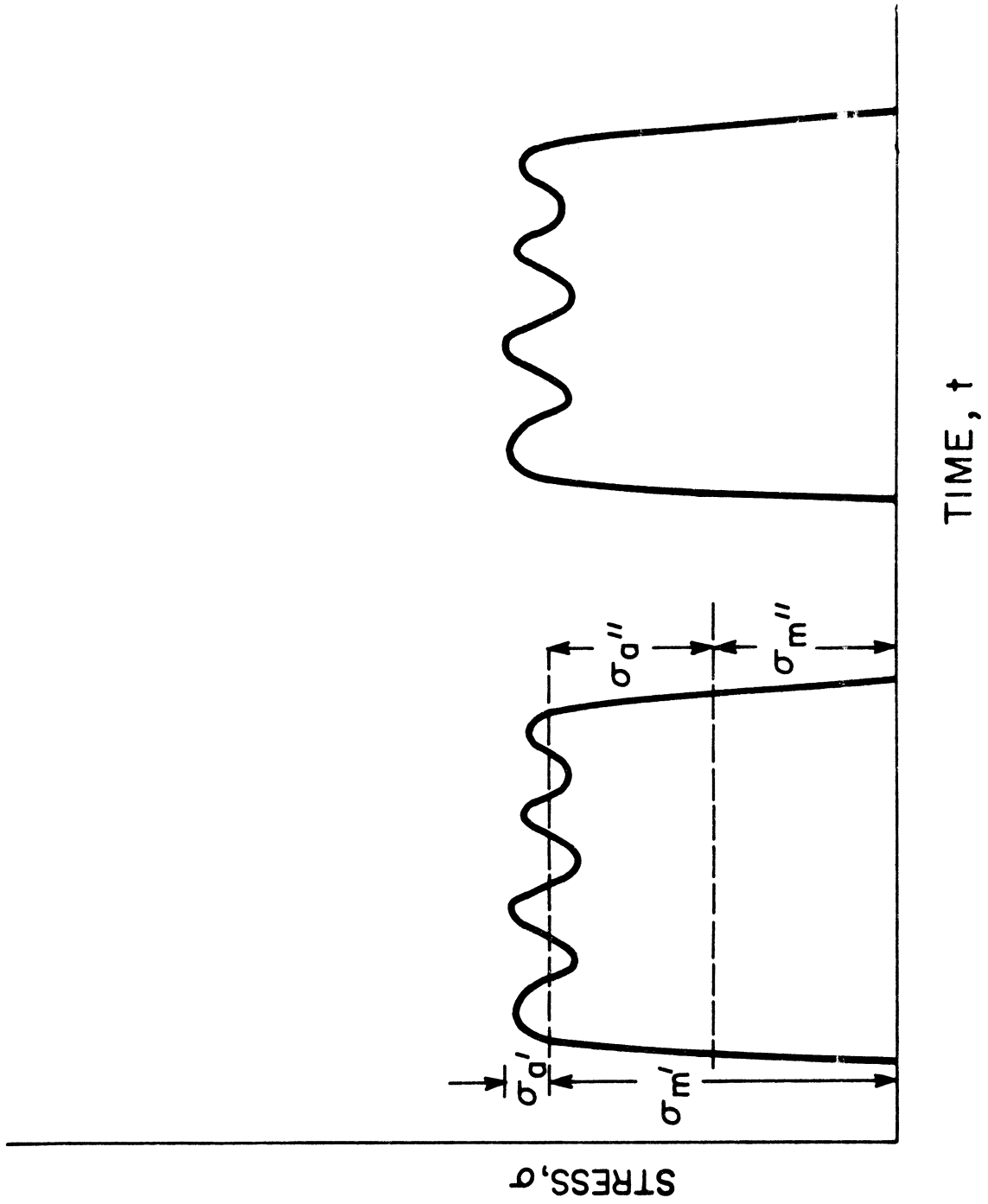


Fig. 6. The Variation of the Stress with Time at the Liquid Droplet-Coat Interface.

The equivalent dynamic stresses corresponding to the two modes of stress oscillations just described may thus be written as

$$\sigma'_e = \frac{\sigma |\psi_{sc}| \sigma_u}{\sigma_u - \sigma} \quad (45)$$

$$\sigma''_e = \frac{(\sigma/2) \sigma_u}{\sigma_u - \sigma/2} \quad (46)$$

The number of cycles for which the material at point B is subjected to a given stress between  $\sigma_e$  and  $\sigma_e + d\sigma_e$  is equal to the number of impacts on a  $dr$  wide annulus located at  $r$  (Fig. 7). During the incubation period the total number of impacts on the annulus is

$$f_i = n_i 2\pi r dr \quad (47)$$

For each single impact the number of stress oscillations in the coating is  $\bar{k}$  (equation 29). The total number of stress oscillations during  $f$  impact is, therefore,  $\bar{k}f_i$ . Accordingly, Miner's rule becomes

$$\sum_i \left( \frac{f_i}{N'_i} + \frac{\bar{k} f_i}{N''_i} \right) = a_1 \quad (48)$$

where  $N'_i$  is the fatigue life for overstress levels at  $\sigma'_e$  and  $N''_i$  is the fatigue life for overstress levels at  $\sigma''_e$ .

Since  $r$  varies continuously from zero to infinity, equations (47) and (48) may be written as

$$\int_0^{\infty} \frac{n_i 2\pi r}{N'_i} dr + \int_0^{\infty} \frac{\bar{k} n_i 2\pi r}{N''_i} dr = a_1 \quad (49)$$

The first term on the left hand side represents the stress oscillation about  $\sigma_m = \sigma/2$  and the second term the oscillation about  $\sigma_m = \sigma$ . From

equation (41)  $rdr$  is

$$rdr = -\frac{1}{2\pi} \frac{\bar{F}(1-2\nu_c)}{2\sigma^2} d\sigma \quad (50)$$

$d\sigma$  is determined by differentiating equations (45) and (46)

$$d\sigma = \left[ \frac{|\psi_{sc}| (\sigma_{uc})^2}{[(\sigma_{uc}) - \sigma]^2} \right]^{-1} d\sigma'_e \quad (51)$$

$$d\sigma = \left[ \frac{2(\sigma_{uc})^2}{[2(\sigma_{uc}) - \sigma]^2} \right]^{-1} d\sigma''_e \quad (52)$$

Substitution of equations (50-52) into equation (49) results in

$$-\int_{\sigma_u}^{\sigma_I} \frac{2\pi n_1 \bar{F} \frac{(1-2\nu_c)}{2\pi (4\sigma_e^2)}}{N'} d\sigma'_e - \int_{\sigma_u}^{\sigma_I} \frac{\bar{k} 2\pi n_1 \bar{F} \frac{|\psi_{sc}| (1-2\nu_c)}{4\pi \sigma_e''^2}}{N''} d\sigma''_e \quad (53)$$

The lower and upper limits of the integrals have been changed to the ultimate tensile strength  $\sigma_u$  and the endurance limit  $\sigma_I$ , respectively.

In order to perform the integration the fatigue life  $N$  must be known as a function of the stress  $\sigma_e$ . For most materials the fatigue curve between  $\sigma_u$  and  $\sigma_I$  may be approximated by (Fig. 9)

$$N = b_1 \sigma_e^{-b} \quad (54)$$

where  $b_1$  and  $b$  are constants. Equation (54) must satisfy the conditions

$$N_1 = 1 \quad \text{for} \quad \sigma_e = \sigma_u \quad (55a)$$

$$N = 10^{b_2} \quad \text{for} \quad \sigma = \sigma_I \quad (55b)$$

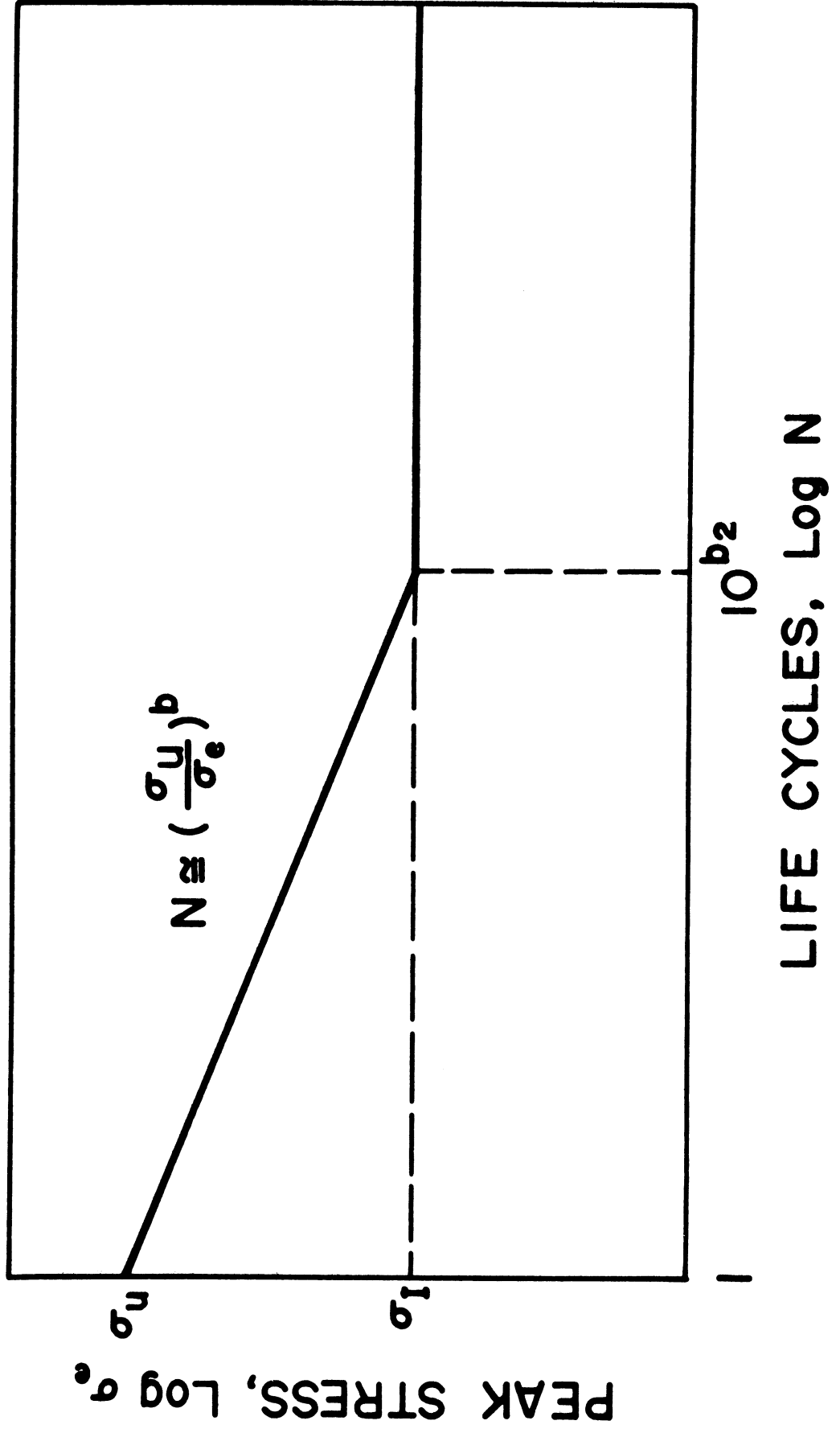


Fig. 9. Idealized  $\sigma_e$ -N Curve

In equation (55b),  $10^{b_2}$  corresponds to the "knee" in the fatigue curve (Fig. 9). Equations (54) and (55) yield

$$N = (\sigma_u / \sigma_e)^b \quad (56)$$

$$b = \frac{b_2}{\log_{10} \left( \frac{\sigma_{uc}}{\sigma_{Ic}} \right)} \left( \frac{\sigma_{uc}}{\sigma_{Ic}} \right)^{b-1} \quad (57)$$

Substituting equations (56) and (36) into equation (53) and integrating we obtain

$$\frac{\pi d^2}{4} n_i \bar{\sigma}^{-o} (1-\nu_c) \frac{\sigma_{uc}^{b-1} \sigma_{Ic}^{b-1}}{4(b-1)\sigma_{uc}^b} (1 + 2 |\psi_{sc}| \bar{k}) = a_1 \quad (58)$$

Introducing the definitions

$$S = \frac{4\sigma_u (b-1)}{(1-2\nu_c) \left[ 1 - \left( \frac{\sigma_{Ic}}{\sigma_{uc}} \right)^{b-1} \right]} \approx \frac{4(\sigma_{uc})^{b-1}}{1-2\nu_c} \quad (59)$$

$$S_e = \frac{S}{1 + 2\bar{k} |\psi_{sc}|} \quad (60)$$

$$n_i^* = n_i \frac{\pi d^2}{4} \quad (61)$$

equation (58) becomes

$$n_i^* = a_1 \frac{S_e}{\bar{\sigma}^{-o}} \quad (62)$$

The parameter  $S_e$  characterizes the "strength" of the material. Thus, the number of impacts needed to initiate damage is proportional to the ratio of the "strength" of the material  $S_e$  to the stress  $\bar{\sigma}^{-o}$  produced by

the impinging droplets. Such a dependence of  $n_i^*$  on  $S_e$  and  $\bar{\sigma}^0$  is reasonable, since the length of the incubation period is expected to increase with increasing  $S_e$  and with decreasing  $\bar{\sigma}^0$ . However, in view of the fact that equation (62) is based on the fatigue properties of materials in pure torsion and bending, one cannot expect a linear relationship to hold between  $n_i^*$  and  $S_e/\bar{\sigma}^0$ . In order to extend the range of applicability of equation (62), while retaining its major feature (namely the functional dependence of  $n_i^*$  on  $S_e/\bar{\sigma}^0$ ) we write

$$n_i^* = a_1 \left( \frac{S_e}{\bar{\sigma}^0} \right)^{a_2} = a_1 \left[ \frac{S}{\bar{\sigma}^0} \frac{1}{1 + 2\bar{k}|\psi_{sc}|} \right]^{a_2} \quad (63)$$

where both  $a_1$  and  $a_2$  are as yet undetermined constants.

For a homogeneous material (in the absence of coating) the incubation period is (Reference 13)

$$n_{iH}^* = a_1 \left( \frac{S}{P} \right)^{a_2} \quad (64)$$

Both  $P$  and  $\bar{\sigma}^0$  denote an average stress at the surface. Note, that  $n_i^*$  and  $n_{iH}^*$  differ only by the factor  $1/(1+2\bar{k}|\psi_{sc}|)$ . This factor represents the damping effect of the coating.

A homogeneous material may be viewed as either a material with very thick coating ( $h/d \rightarrow \infty$ ,  $\bar{k} \rightarrow 0$ , equation 30), or one in which the coating and the substrate are made of the same material ( $\psi_{sc} = 0$ , equation 13). It is evident that for either one of these conditions equation (63) reduces to equation (64), provided that the constants  $a_1$  and  $a_2$  have the appropriate values. To ensure that in the limits ( $\bar{k} \rightarrow 0$  and/or  $\psi_{sc} \rightarrow 0$ ) equations (63) and (64) become equal we adopt here the same values for

$a_1$  and  $a_2$  as were derived by Springer and Baxi (Reference 13) for homogeneous materials.\* Using the values  $a_1=7.1 \times 10^{-6}$  and  $a_2=5.7$  we obtain

$$n_i^* = 7.1 \times 10^{-6} \left( \frac{S_e}{\bar{\sigma}^0} \right)^{5.7} \quad (65)$$

Equation (65) gives the incubation period of a single layer of coating of arbitrary thickness. The validity of the model must now be evaluated by comparing this result to experimental data. The comparison is presented in Fig. 10. In this figure all the data are included for which both  $n_i$  and the relevant material properties ( $\sigma_u, \sigma_I, b_2, \nu, E, \rho$  for both the coating and the substrate were available. As can be seen, there is excellent correlation between the model and the data, lending support to the validity of the model.

As was discussed in Section II, the present model is valid only when the incubation time is greater than zero. This condition is met when  $n_i^* > 1$  or, according to equation(65), when  $S_e / \bar{\sigma}^0 > 8$ . Thus, an incubation period exists if

$$\begin{aligned} n_i^* &> 1 \\ S_e / \bar{\sigma}^0 &> 8 \end{aligned} \quad (66)$$

When  $S_e / \bar{\sigma}^0$  is equal to or less than 8 damage will occur even upon one impact per site. This is most likely to occur at high impact velocities in which case  $\bar{\sigma}^0$  is high (since  $\sigma^0 \sim P \sim V$ ).

---

\* The value for the constant  $a_1$  was given in Reference 13 as  $3.7 \times 10^{-4}$ . This value was obtained by using the stress  $\sigma$  instead of  $\sigma_e$  in calculating the fatigue life. When  $\sigma$  is replaced by  $\sigma_e$   $a_1$  becomes  $7.1 \times 10^{-6}$  (see Appendix II).

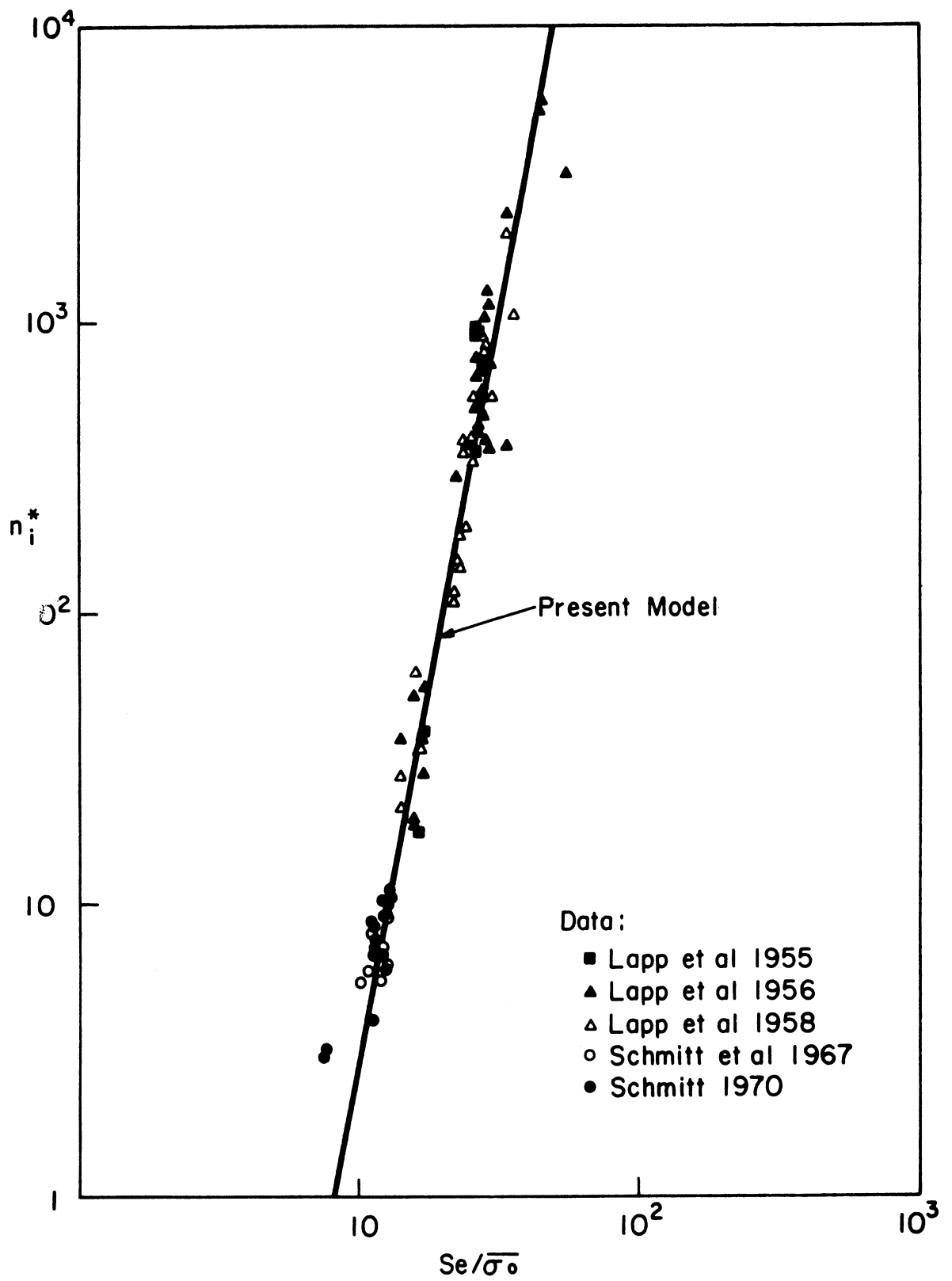


Fig. 10. Incubation Period  $n_i^*$  versus  $S_e/\bar{\sigma}^0$ . Solid Line: Model (Eq. 65). Symbols Defined in Table 1.



## SECTION V

### RATE OF MASS REMOVAL

The mass removal rate of coat-substrate systems can be calculated in a manner analogously to the mass removal rate of homogeneous materials. The analysis relevant to homogeneous materials is given in Reference 13. Parts of this analysis will be repeated here for the sake of completeness, and to enable the reader to follow the discussion without the need of constant referral to the earlier reference.

Beyond the incubation period, erosion of the surface of the material (as expressed in terms of mass loss) proceeds at a nearly constant rate as shown in Fig. 2b. In order to calculate this erosion rate, an analogy is drawn again between the behavior of the material upon which liquid droplets impinge, and the behavior of specimens subjected to torsion or bending fatigue tests. Experimental observations show that in the latter case the specimens do not all fail at once at some "minimum life", but their failure is scattered around a "characteristic life". For specimens in torsion and bending tests the probability that failure will occur between minimum life  $n_1$  and any arbitrary longer life  $n$  may be estimated from the Weibull distribution (Reference 25)

$$p = 1 - \exp\left[-\left(\frac{n-n_1}{n_a}\right)^\beta\right] \quad (67)$$

where  $n_a$  is the characteristic life corresponding to the 63.2 percent failure point and  $\beta$  is a constant (Weibull slope). For  $(n-n_1)/n_a \ll 1$  equation (67) may be approximated by

$$p = \left(\frac{n-n_1}{n_a}\right)^\beta \quad (68)$$

The probability  $p$  can also be taken as the number of specimens that fail between  $n_i$  and  $n$ . If the material undergoing erosion due to liquid impingements is considered to be made up of many small "parts", then the amount of material eroded (mass loss) is proportional to  $p$ , i.e.

$$\frac{m}{\rho d} = a_3 \left( \frac{n-n_i}{n_a} \right)^\beta = a_3 \left( \frac{n^*-n_i^*}{n_a^*} \right)^\beta \quad (69)$$

$\rho$  is the density of the material being eroded. In equation (69)  $m$  was nondimensionalized with respect to  $\rho d$  in order to render the proportionality constant  $a_3$  dimensionless. Equation (6b) is now rewritten in dimensionless form

$$\frac{m}{\rho d} = \frac{\alpha}{\pi \rho d^{3/4}} (n^*-n_i^*) \quad (70)$$

Equations (69) and (70) give

$$\frac{\alpha}{\pi \rho d^{3/4}} = a_3 \frac{(n^*-n_i^*)^{\beta-1}}{(n_a^*)^\beta} \quad (71)$$

According to equation (71) the mass loss rate  $\alpha$  depends on the total number of impacts  $n$ . However, our model postulates a constant mass loss rate (i.e.  $\alpha$  is independent of  $n$ , see Fig. 2b), at least when  $n_i < n < n_f$ . This requirement can be met by setting  $\beta=1$ . Such a value for  $\beta$  is not unreasonable under high frequency loading (Reference 21). The characteristic life  $n_a$  is related to the minimum life  $n_i$ . This relationship may be expressed suitably as

$$n_a^* = a_4 n_i^* \quad (72)$$

where  $a_4$  and  $a_5$  are constants. Introducing the dimensionless mass loss rate

$$\alpha^* = \frac{\alpha}{\pi \rho \bar{d}^3 / 4} \quad (73)$$

equations (71-73), together with the assumption  $\beta=1$  yield

$$\alpha^* = a_3 \frac{1}{(n_i^*)^{a_6}} \quad (74)$$

The  $\alpha^*$  given by equation (74) applies to both homogeneous materials and to coat-substrate systems. For homogeneous materials the values of  $a_3$  and  $a_6$  were determined by Springer and Baxi (Reference 13) and were found to be  $a_3=0.023$  and  $a_6=0.7$ . Similarly as for the incubation period, we adopt the same values of these constants for the present problem of homogeneous substrates covered by a single layer of coating, i.e.

$$\alpha^* = 0.023 \frac{1}{(n_i^*)^{0.7}} \quad (75)$$

In the case of  $\bar{k} \rightarrow 0$  and/or  $\psi_{sc} \rightarrow 0$  the incubation period  $n_i^*$  reduces to  $n_{iH}^*$  (see Section IV). Consequently, under these conditions,  $\alpha^*$  (given by equation 75) becomes the same as given by Springer and Baxi's formula for homogeneous materials.

The validity of the foregoing model was assessed by comparing  $\alpha^*$ , calculated by equation (75) to available experimental data. This comparison, given in Fig. 11, shows very good agreement between the calculated and measured  $\alpha^*$  values. This lends further confidence to the model.

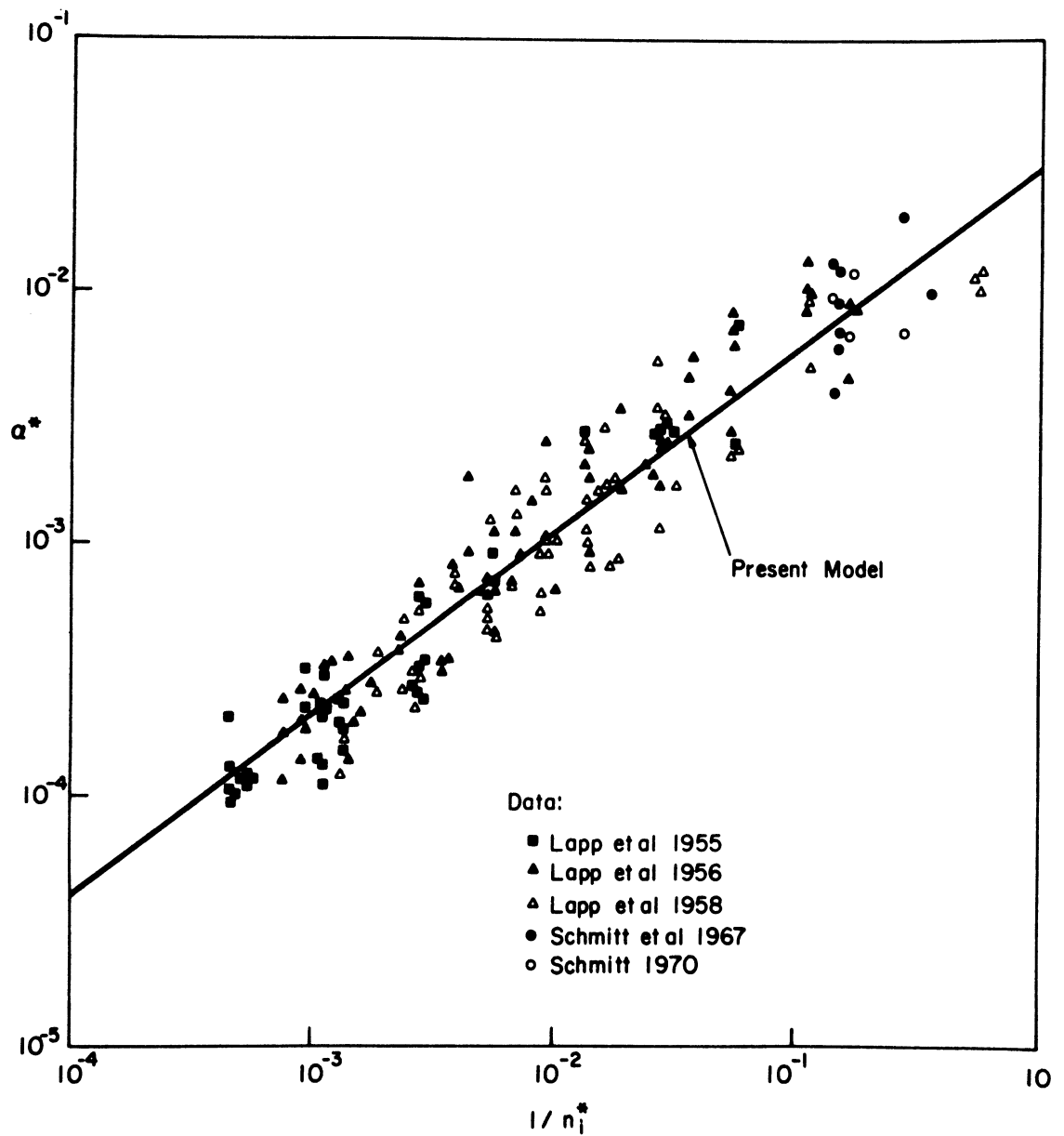


Fig. 11. Rate of Erosion Versus the Inverse of the Incubation Period. Solid Line: Model (Eq. 75). Symbols Defined in Table 1.

## SECTION VI

### TOTAL MASS LOSS

The total mass loss was given by equation (6b) as

$$m = \alpha(n - n_i) \quad (6b)$$

Introducing the dimensionless parameter

$$m^* = \frac{m}{\rho_c d} \quad (76)$$

equations (6b), (70) and (73) yield

$$m^* = \alpha^* (n^* - n_i^*) \quad (77a)$$

or

$$\frac{m^*}{\alpha^*} = n^* - n_i^* \quad (77b)$$

According to equation (77b) it should be possible to correlate all erosion data on a  $m^*/\alpha^*$  versus  $(n^* - n_i^*)$  plot. Therefore, we have included all the existing data on such a plot (Fig. 12). In this figure the theoretical result given by our model (equation 77a) is also indicated. The agreement between the model and the data is quite good, particularly in view of the large errors inherent in many of the measurements.

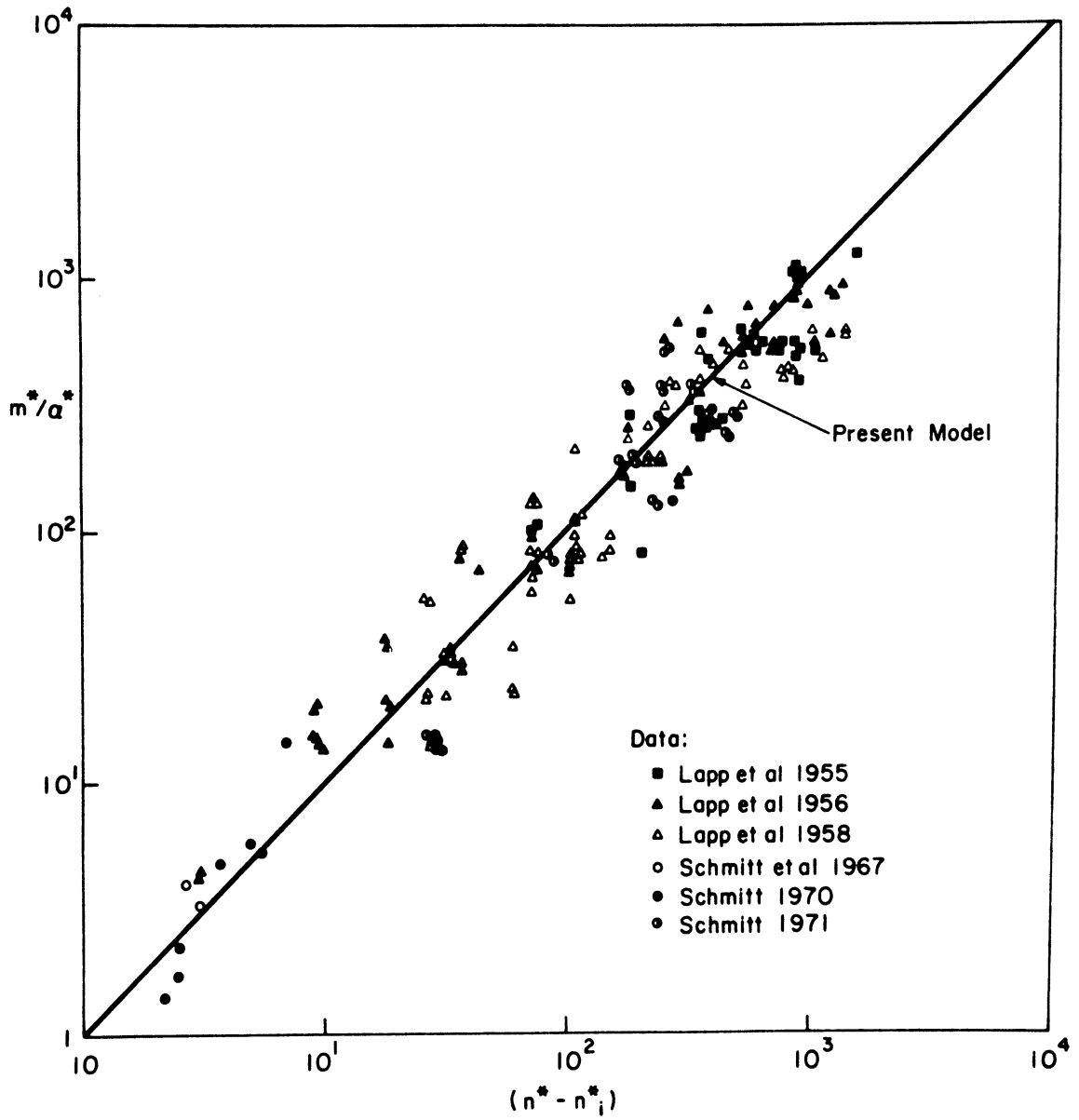


Fig. 12. Comparison of Present Model (Solid Line, Eq. 77b) with Experimental Results. Symbols Defined in Table 1.

## SECTION VII

### LIMITS OF APPLICABILITY OF MODEL

The results presented in Sections II-VI are valid when (a) there is a finite incubation period, and (b) the mass loss varies linearly either with time  $t$  or with the number of impacts  $n$ . The first of this condition is met when the following inequality is satisfied (see equation 66)

$$n_i^* > 1 \tag{66a}$$

According to equation (65) this condition may also be expressed as

$$S_e / \bar{\sigma}_o > 8 \tag{66b}$$

Equations (66a) or (66b) provide the lower limit of the applicability of the model. The upper limit beyond which the present model cannot be applied is determined by the second condition given above, namely that the mass loss must vary linearly with  $t$  or  $n$ . An estimate of this limit was made by observing that up to about  $n=3n_i$  the data obtained at various values of  $n$  did not show any systematic deviation from the model. Thus, the results are valid as long as the number of impacts is less than three times the incubation period, i.e.

$$n < 3n_i \tag{78a}$$

or in dimensionless form

$$n^* < 3n_i^* \tag{78b}$$

Using equation (65) we obtain the following expression for the upper limit

$$n < 21.3 \times 10^{-6} \left( \frac{S_e}{\sigma} \right)^{5.7} \quad (78c)$$

Note that the two limits expressed by equations (66) and (78) do not impose any constraints on either the material or the impact velocity. Thus, the results are valid for any material and for any velocity, provided that the experimental conditions fall within the range specified by equations (66) and (78).



## SECTION VIII

### FATIGUE FAILURE OF THE SUBSTRATE

The foregoing analysis was based on the assumption that the coating fails before the substrate. Under some conditions, however, the substrate may fail before the coating. The analyses presented in Sections IV, V and VI can be applied readily to such a situation. To calculate the behavior and failure of the substrate only minor modifications need be made in the previous results. The average stress at the surface of the coating  $\bar{\sigma}^0$  (equation 34a) must be replaced by the average stress at the coat-substrate interface  $\bar{\sigma}^h$  (equation 34b). Consequently, equation (62) must be written as

$$n_i^* = a_1 \frac{S_e}{\bar{\sigma}^h} \quad (79)$$

Furthermore, in calculating  $S_e$  (equation 59) the parameters  $(\sigma_{u_c})$ ,  $(\sigma_{l_c})$  and  $\nu_c$  must be replaced by the properties of the substrate  $(\sigma_{u_s})$ ,  $(\sigma_{l_s})$  and  $\nu_s$ . All other results remain unaltered.

SECTION IX  
COMPARISON BETWEEN THE RESULTS OF THE  
UNIAXIAL STRESS AND STRAIN THEORIES

It was discussed in Section III that the stresses in the coating may be evaluated by assuming either uniaxial (one dimensional) stress waves or uniaxial (one-dimensional) strain waves propagating through the material. The uniaxial stress wave model was applied to the problem by Conn et al (References 10, 11) and by Engel and Piekutowski (Reference 8). The uniaxial strain model was employed by Morris (Reference 7). There has been considerable speculation in the literature (References 16, 26, 27) as to which approach yields more accurate results. Here, we examine briefly the differences in the uniaxial stress and strain models. These differences can best be illustrated using a graphical solution method (Reference 7). First let us consider the impact of a droplet on a homogeneous (uncoated) material. Upon impact one dimensional stress waves propagate into the solid and the liquid with velocities  $v_s$  and  $v_L$ , respectively. The stress at any point behind the wave front in either the solid or in the liquid is given by

$$\sigma = \rho v u \tag{80}$$

where  $u$  is the particle velocity at the point and  $\rho$  is the density of the material. The wave velocity  $v$  is specified by the relationship

$$v = C + B_1 u + B_2 u^2 \tag{81}$$

$C$  is the velocity of the sound in the material.  $B_1$  and  $B_2$  are constants. The  $\sigma$  versus  $u$  curve, shown in Fig. 13, is called the Rankine-Hugoniot

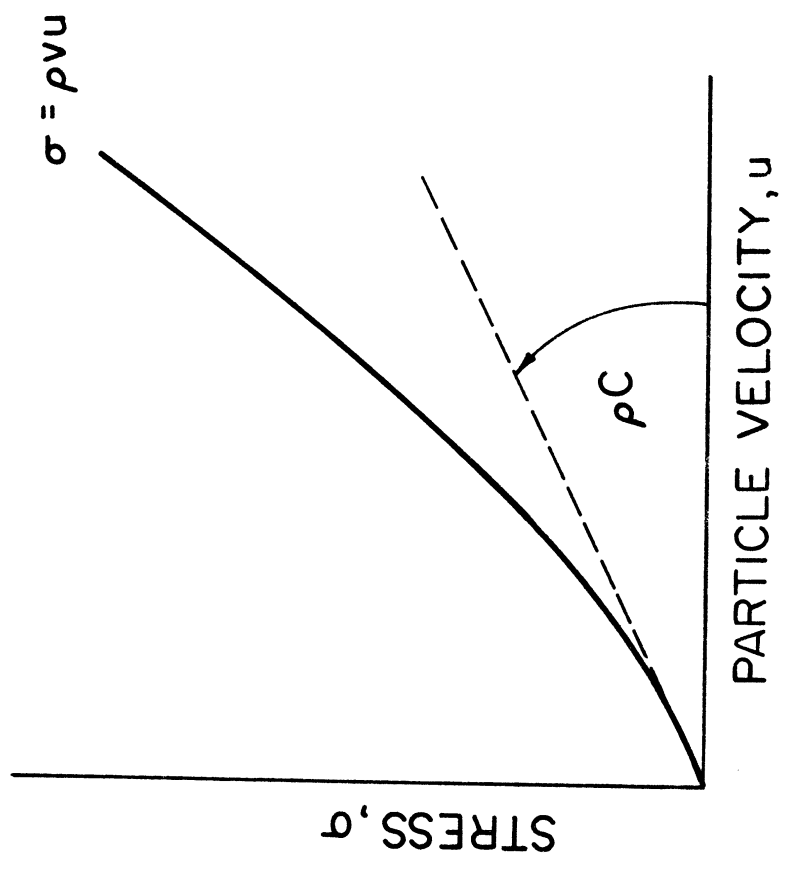


Fig. 13. Rankine-Hugoniot Curve for a Homogeneous Solid.

curve. Note that the slope of the curve at the origin ( $u=0$ ) is the dynamic impedance  $\rho C$ . The slope of the curve at  $u>0$  is always larger than  $u=0$ .

It is assumed now that at the liquid-solid interface the displacements of the liquid and solid surfaces are equal (perfect contact). Then, if the particle velocity at the interface is denoted by  $u_0$ , then the stresses at the interface are (see equation 80)

$$\sigma_s = \rho_s v_s u_0 \quad (\text{solid}) \quad (82)$$

$$\sigma_L = \rho_L v_L (V - u_0) \quad (\text{liquid}) \quad (83)$$

Since  $\sigma_s = \sigma_L$  the intersection of the  $\sigma_s$  versus  $u_0$  and  $\sigma_L$  versus  $u_0$  curves (i.e. the Rankine-Hugoniot curves for the solid and the liquid) yield the stress  $\sigma_\infty$  and the particle velocity  $u_1$  at the interface (Fig. 14).

In the uniaxial stress model proposed by Conn (References 10, 11)  $v$  is taken to be constant and equal to  $C$ , i.e.  $B_1=B_2=0$  for both the liquid and the solid. In the uniaxial strain wave model described by Morris (Reference 7)  $v$  is a function of  $u_0$  (equation 81). The uniaxial stress model yields a lower stress at the interface than the uniaxial strain model, as indicated in Fig. 14. In this figure, and in the subsequent discussions the superscript B implies stresses evaluated by the uniaxial stress model ( $B_1$  and  $B_2$  are not zero).

The foregoing procedure can be extended to a substrate covered by a thin layer of coating (Reference 7). The Rankine-Hugoniot relationships

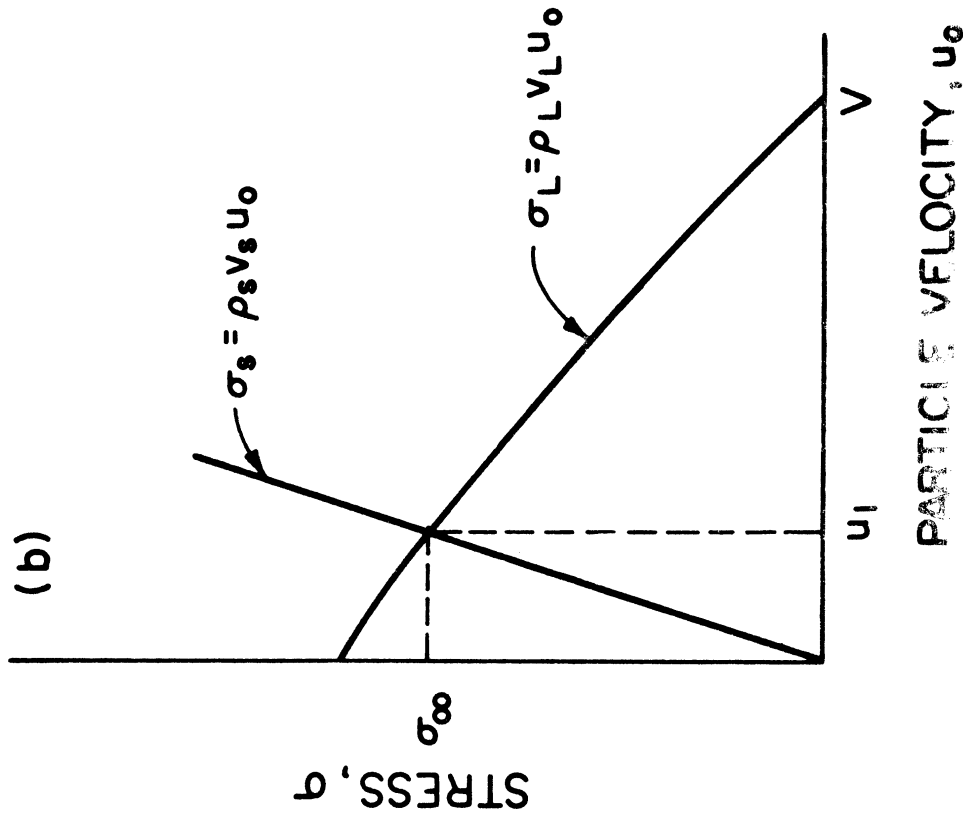
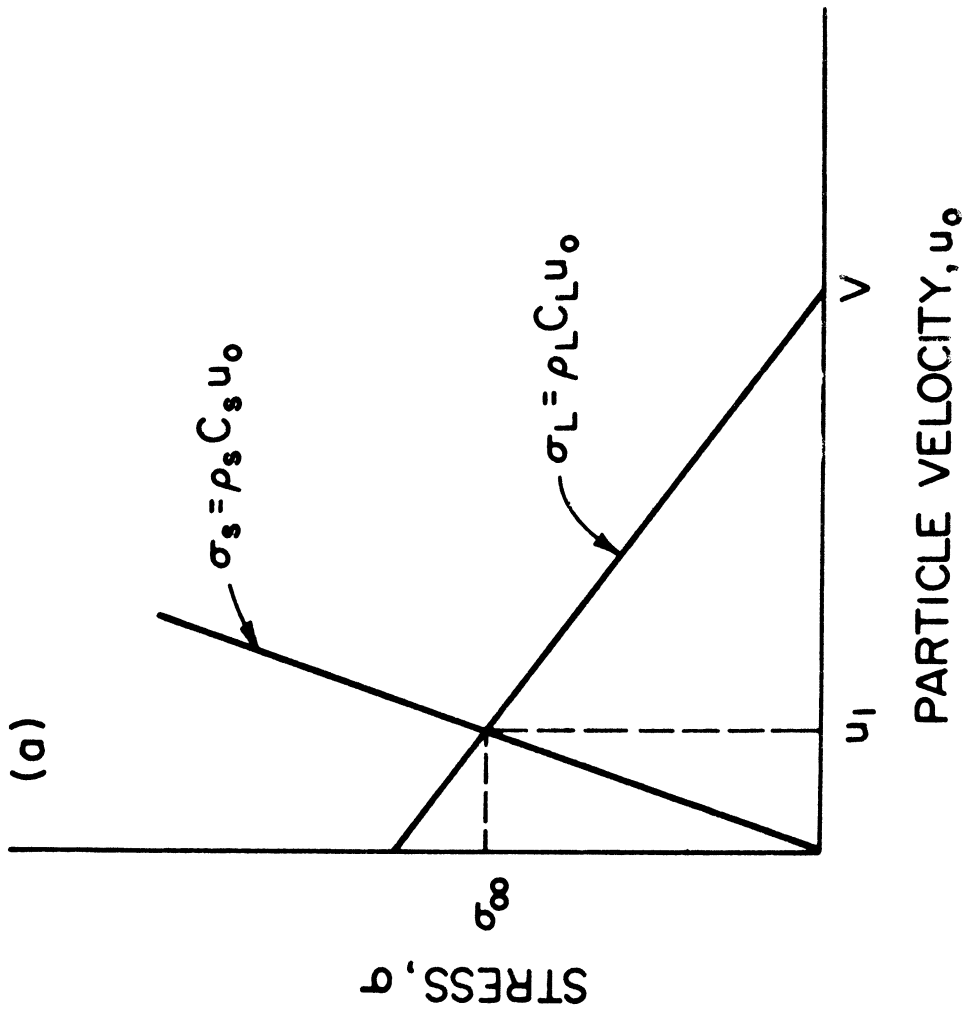


Fig. 14. Impact of the Droplet on a Homogeneous Material. Calculation of the Stress at the Liquid-Solid Interface by (a) the Uniaxial Stress Wave Model and (b) the Uniaxial Strain Wave Model.

for the coating and the liquid

$$\sigma_c = \rho_c v_c u_o \quad (\text{curve 1}) \quad (84)$$

$$\sigma_L = \rho_L v_L (V - u_o) \quad (\text{curve 2}) \quad (85)$$

are drawn on a  $\sigma_1$  versus  $u_o$  plot. The intercept of these curves yields the stress  $\sigma_1$  and the particle velocity  $u_1$  at surface of the coating ( $x=0$ ). Equation (84) is based on the properties of the undisturbed coating. The Rankine Hugoniot relationship for the coating behind the stress wave is

$$(\sigma_c - \sigma_1) = \rho_c v_c (u_1 - u_o) \quad (\text{curve 3}) \quad (86)$$

Finally, for the substrate we have

$$\sigma_s = \rho_s v_s u_o \quad (\text{curve 4}) \quad (87)$$

Curves (3) and (4) are also drawn on the  $\sigma$  versus  $u_o$  plot. The intercepts of curves (3) and (4) and (2) and (4) give  $\sigma_2$  and  $\sigma_\infty$ , respectively. Construction of a typical  $\sigma$  versus  $u_o$  plot is illustrated in Fig. 15. Figure 15a shows the results for the uniaxial stress theory ( $v_L = C_L$ ,  $v_c = C_c$ ,  $v_s = C_s$ ) for the condition

$$\rho_L C_L > \rho_c C_c < \rho_s C_s \quad (88)$$

For the uniaxial strain model the wave velocities  $v_L$ ,  $v_c$  and  $v_s$  are not constants. However, if the condition

$$\rho_L v_L > \rho_c v_c < \rho_s v_s \quad (89)$$

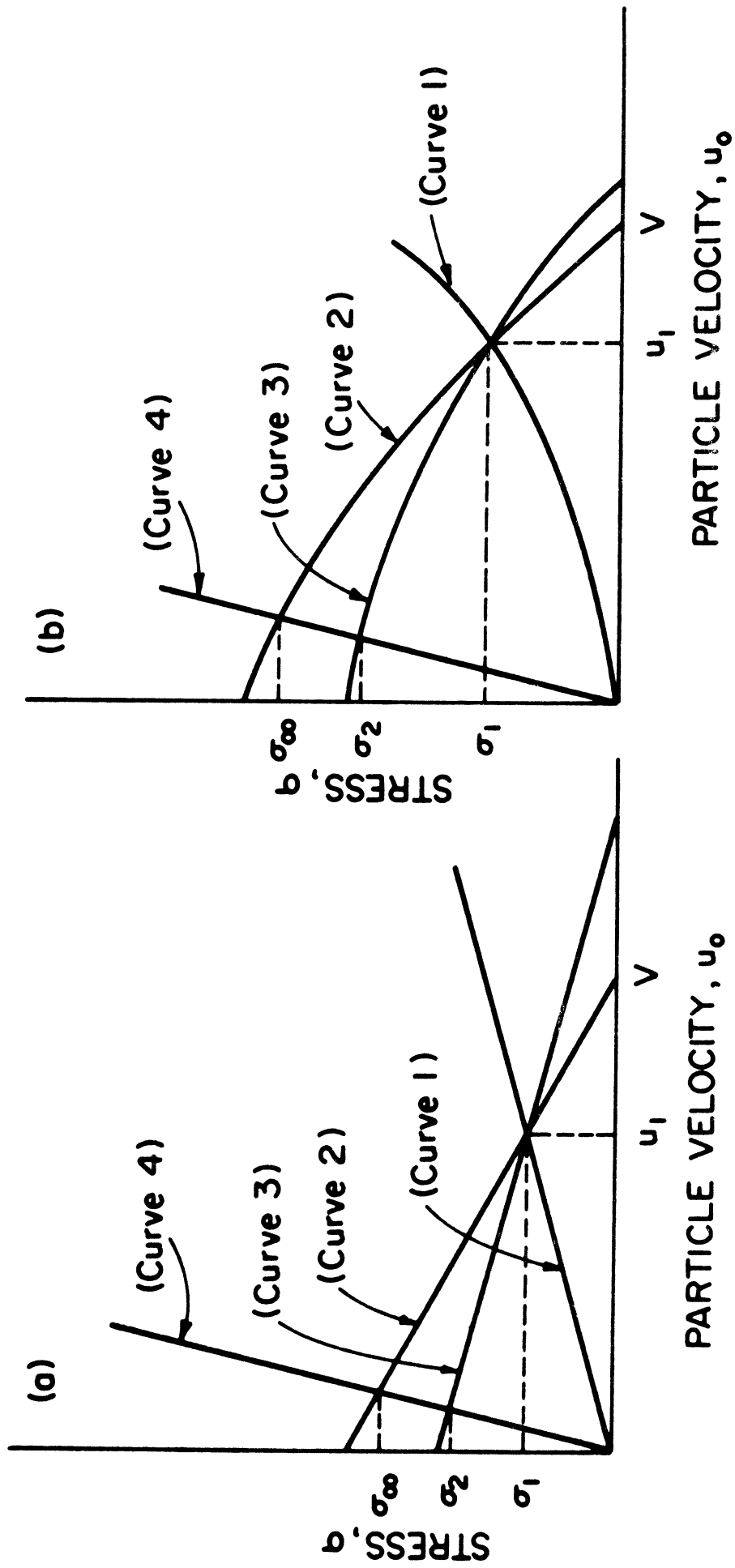


Fig. 15. Impact of a Droplet on a Substrate Covered with a Single Layer of Coating. Calculation of the Stress at the Liquid-Coating Interface  $\sigma_1$ , the Stress at the Coating-Substrate Interface  $\sigma_2$ , and the Stress that Would Occur on the Surface of the Substrate in the Absence of Coating  $\sigma_\infty$ . (a) Uniaxial Stress Wave Model; (b) Uniaxial Strain Wave Model.

is satisfied for each value of  $u_0$  then the Rankine-Hugoniot curves are as shown in Fig. 15b. Thus, as long as the condition in equation (89) is satisfied  $\sigma_2^B < \sigma_\infty^B$ . This is in agreement with the result of the uniaxial stress wave model. If the condition expressed by equation (89) is not satisfied for all values of  $u_0$  then  $\sigma_2^B$  may be larger than  $\sigma_\infty^B$ . Whether  $\sigma_2^B$  is larger or smaller than  $\sigma_\infty^B$ , depends on the relative magnitudes of  $B_1$  and  $B_2$  for the liquid, the coating and the substrate. The conditions under which this might occur cannot be specified at present time, because values for  $B_1$  and  $B_2$  are unavailable for most materials.

Plots similar to those presented in Fig. 15 could also be drawn for materials with different relative impedances (i.e.  $\rho_L v_L < \rho_C v_C < \rho_S v_S$ ,  $\rho_L v_L < \rho_C v_C > \rho_S v_S$ ,  $\rho_L v_L > \rho_C v_C < \rho_S v_S$ ; see Fig. 4). However, the conclusions presented in the foregoing would not be altered.

It is noted here that curves (3) and (1) in Fig. 15 are symmetric with respect to  $\sigma = \sigma_1$ , regardless of the values of  $B_1$  and  $B_2$ . This symmetry was not satisfied by the Rankine-Hugoniot plot presented in Reference 7.



SECTION X

SUMMARY

The following formulae may be used to estimate the incubation time and the mass loss of the coat material of coat-substrate systems subjected to repeated impingement of liquid droplets.

a) Incubation Period

$$n_i^* = 7.1 \times 10^{-6} \left[ \frac{S_e}{\bar{\sigma}} \right]^{5.7} \quad (90)$$

or

$$n_i = \frac{9.05 \times 10^{-6}}{d^2} \left[ \frac{S_e}{\bar{\sigma}} \right]^{5.7} \quad \left( \frac{\text{no. of impact}}{\text{unit area}} \right) \quad (91)$$

or

$$t_i = \frac{9.05 \times 10^{-6}}{q V \cos \theta d^2} \left[ \frac{S_e}{\bar{\sigma}} \right]^{5.7} \quad (\text{time}) \quad (92)$$

where

$$S_e = \frac{4\sigma_u (b-1)}{(1-2\nu_c) [1 + 2 \bar{k} |\psi_{sc}|]} \quad (93)$$

$$\bar{\sigma} = \frac{\rho_L C_L V \cos \theta}{1 + \frac{\rho_L C_L}{\rho_c C_c}} \frac{1 + \psi_{sc}}{1 - \psi_{sc} \psi_{Lc}} \left[ 1 - \psi_{sc} \frac{1 + \psi_{Lc}}{1 + \psi_{sc}} \frac{1 - \exp(-\gamma)}{\gamma} \right] \quad (94)$$

and

$$\psi_{sc} = \frac{\rho_s C_s - \rho_c C_c}{\rho_s C_s + \rho_c C_c}, \quad \psi_{Lc} = \frac{\rho_L C_L - \rho_c C_c}{\rho_L C_L + \rho_c C_c} .$$

$$\gamma = \frac{C_c}{C_L} \frac{d}{h} [1 - \psi_{sc} \psi_{Lc}] \quad (95)$$

$$\bar{k} = \frac{1}{1 - \psi_{sc} \psi_{Lc}} \left\{ 1 - \exp \left[ - \frac{C_c}{C_L} \frac{d}{h} (1 - \psi_{sc} \psi_{Lc}) \right] \right\}$$

b) Rate of Mass Removal

$$\alpha^* = 92 \left[ \frac{\bar{\sigma}^o}{S_e} \right]^4 \quad (96)$$

or

$$\alpha = 70.6 \rho_c d^3 \left[ \frac{\bar{\sigma}^o}{S_e} \right]^4 \quad \left( \frac{\text{mass loss}}{\text{impact}} \right) \quad (97)$$

$S_e$  and  $\bar{\sigma}^o$  are defined in equations (93) and (94).

c) Total Mass Loss

$$m^* = \alpha^* (n^* - n_i^*) \quad (98)$$

or

$$m = \alpha (n - n_i) \quad \left( \frac{\text{mass loss}}{\text{unit area}} \right) \quad (99)$$

Equations (91), (97) and (99) yield the mass loss per unit area in time  $t$

$$m = 70.6 \rho_c d^3 \left[ \frac{\bar{\sigma}^o}{S_e} \right] \left\{ (q t V \cos \theta) - \frac{9.05 \times 10^{-6}}{d^2} \left( \frac{S_e}{\bar{\sigma}^o} \right)^{5.7} \right\} \quad (100)$$

$S_e$  and  $\bar{\sigma}^o$  are defined as in equations (93) and (94).

The foregoing results are subject only to the following two constraints.

a) Incubation time must be greater than zero ( $t_i > 0$ ), a requirement satisfied by the condition

$$\frac{S_e}{\bar{\sigma}^o} > 7.96 \quad (101)$$

b) Total time elapsed must be less than three times the incubation period, i.e.

$$\begin{aligned}
 t &< 3t_i \\
 n &< n_i \\
 n_i^* &< 3n_i^*
 \end{aligned}
 \tag{102}$$

or

$$\frac{3}{2} \frac{(V \cos \theta) I t}{V_t d^3} < 2.13 \times 10^{-5} \left[ \frac{S_e}{\bar{\sigma}^0} \right]^{5.7}
 \tag{103}$$

$S_e$  and  $\bar{\sigma}^0$  are defined in equations (93) and (94).

TABLE 1. Description of Data and Symbols Used in Figures 10, 11 and 12\*

Symbol	Investigator	Coating	Substrate	Coating Thickness mils	Velocity ft/sec	Intensity (in/hr)	Drop Size mm
■	Lapp et al 1955	Neoprene	Polyester Aluminum Steel Aluminum	8.9, 10	731	1	1.9
				15, 20			
				20			
▲	Lapp et al 1956	Teflon	Aluminum	5, 10	731		
△	Lapp et al 1958	Neoprene	Polyester Aluminum	4-5, 7, 10, 20	877	1	1.9
				15-17	877		
				Polyethylene	9-15		
○	Schmitt et al 1967	Aluminum	Epoxy Aluminum Polyester	15-30	731	1	1.9
				8-11			
				10			
○	Schmitt et al 1967	Aluminum	Epoxy Aluminum	10	1596	2.5	1.9
				62.5			
○	Schmitt et al 1967	Aluminum	AlP04 PBI Polyimide Epoxy	20	2360	2.5	1.9
				20, 40	3169		
				30			
○	Schmitt et al 1967	Gaco Polyurethane Teflon Nickel	Epoxy	20			
				26, 30			
				35			
○	Schmitt et al 1967	Gaco Polyurethane Teflon Nickel	Epoxy	10			

TABLE 1 (continued)

Symbol	Investigator	Coating	Substrate	Coating Thickness mils	Velocity ft/sec	Intensity in/hr	Drop Size mm
●	Schmitt 1970	Alumina	Polymide	10	1596	2.5	1.9
			Epoxy	40	2360		
		Gaco	Epoxy	10	2751		
					3169		
		Urethane		10, 15, 20, 30	1596		
		Polyethylene	Epoxy		2360		
Nickel	Polymide		2751				
◐	Schmitt 1971	Urethane	Aluminum	15	731	1	1.9
		Neoprene	Epoxy Aluminum	22			

\* Material properties used in obtaining Figs. 10-12 are from References (6), (9)-(10)

APPENDIX I

DERIVATION OF EQUATION (18)

After k number of wave reflections the stress at the coat-substrate interface is (equation 16)

$$\sigma_{2k} = \sigma_1 \frac{1 + \psi_{sc}}{1 - \psi_{sc} \psi_{Lc}} [1 - (\psi_{sc} \psi_{Lc})^k] \quad (\text{A.1.1})$$

After a large number of reflections ( $k \rightarrow \infty$ ) the stress approaches the limit

$$\sigma_{\infty} = \lim_{k \rightarrow \infty} \sigma_{2k} \quad (\text{A.1.2})$$

Noting that

$$\psi_{sc} \psi_{Lc} = \left( \frac{Z_s - Z_c}{Z_s + Z_c} \right) \left( \frac{Z_L - Z_c}{Z_L + Z_c} \right) < 1 \quad (\text{A.1.3})$$

we obtain

$$\lim_{k \rightarrow \infty} (\psi_{sc} \psi_{Lc})^k \rightarrow 0 \quad (\text{A.1.4})$$

Equations (A.1.1), (A.1.2) and (A.1.4) give

$$\frac{\sigma_{\infty}}{\sigma_1} = \lim_{k \rightarrow \infty} \frac{\sigma_{2k}}{\sigma_1} = \frac{1 + \psi_{sc}}{1 + \psi_{sc} \psi_{Lc}} \quad (\text{A.1.5})$$

Using the notations (13) and (14) of Section III, equation (A.1.5) may be written as

$$\sigma_{\infty} = \sigma_1 \frac{1 + Z_L/Z_c}{1 + Z_L/Z_s} = \sigma_1 \frac{Z_L V \cos \theta / (1 + Z_L/Z_s)}{Z_L V \cos \theta / (1 + Z_L/Z_c)} \quad (\text{A.1.6})$$

We now observe that the denominator of equation (A.1.6) is equal to the stress at the surface of the coating [ $P=\sigma_1$ , see equations (4) and (7)].

Thus,  $\sigma_\infty$  is

$$\sigma_\infty = \frac{Z_L V \cos \theta}{1 + Z_L/Z_s} \quad (\text{A.1.7})$$

This is the stress that would be produced on the surface of the substrate if the droplet would impinge upon it directly (see equation 4).

## APPENDIX II

### THE VALUE OF THE CONSTANT $a_1$ FOR HOMOGENEOUS MATERIALS

Springer and Baxi (Reference 13) calculated the incubation period from Miner's rule

$$\frac{f_1}{N_1} + \frac{f_2}{N_2} + \dots + \frac{f_k}{N_k} = a_1 \quad (\text{A.2.1})$$

basing  $N_i$  on the stress  $\sigma$  (equation 10 of Reference 13)

$$\sigma = \frac{F(1-2\nu)}{2\pi r} \quad (\text{A.2.2})$$

Introducing (see equation 11 of Reference 13)

$$f = n_1 2\pi r dr \quad (\text{A.2.3})$$

and (see equation 16 of Reference 13)

$$N = b_1 \sigma^{-b} \quad (\text{A.2.4})$$

Springer and Baxi obtained

$$\int_0^{\infty} \frac{n_1 2\pi r dr}{b_1 \sigma^{-b}} = a_1 \quad (\text{A.2.5})$$

Equation (A.2.2) and (A.2.3) yield

$$r dr = - \frac{1}{2\pi} \frac{F(1-2\nu)}{2\sigma^2} d\sigma \quad (\text{A.2.6})$$

Substitution of equation (A.2.6) into equation (A.2.5) gives

$$- \int_{\sigma_u}^{\sigma_I} \frac{n_1 \left[ \frac{\pi d^2}{4} (1-2\nu) / 2\sigma^2 \right]}{b_1 \sigma^{-b}} d\sigma \quad (\text{A.2.7})$$



Evaluating the integral Springer and Baxi obtained

$$\frac{\pi d^2}{4} n_i = a_1 \frac{S}{P} \quad (\text{A.2.8})$$

where

$$S = \frac{2\sigma_u (b-1)}{\sigma_u^b (1-2\nu) \left[1 - \left(\frac{I}{\sigma_u}\right)\right]} = \frac{2\sigma_u (b-1)}{1-2\nu} \quad (\text{A.2.9})$$

and a constant  $a_2$  was introduced in Springer and Baxi's work

$$n_i \frac{\pi d^2}{4} = a_1 \left(\frac{S}{P}\right)^{a_2} \quad (\text{A.2.10})$$

Comparing equation (A.2.10) with data, Springer and Baxi deduced the values of  $a_1 = 3.7 \times 10^{-4}$  and  $a_2 = 5.7$ , i.e.

$$\frac{\pi d^2}{4} n_i = 3.7 \times 10^{-4} \left(\frac{S}{P}\right)^{5.7} \quad (\text{A.2.11})$$

We compute now the above results basing the fatigue stress  $N$  on the equivalent dynamic stress

$$\sigma_e = \frac{\sigma_a \sigma_m}{\sigma_n - \sigma_m} \quad (\text{A.2.12})$$

Since  $\sigma_a = \frac{\sigma}{2}$  and  $\sigma_m = \frac{\sigma}{2}$ , equation (A.2.12) yields

$$\sigma_e = \frac{\sigma \sigma_u}{2\sigma_u - \sigma} \quad (\text{A.2.13})$$

The replacement of  $\sigma$  by  $\sigma_e$  in equations (A.2.2), (A.2.4) gives

$$\frac{\pi d^2}{4} n_i = a_1 \frac{1}{P} \frac{4 \sigma_u (b-1)}{\sigma_u^{b-1} (1-2\nu) \left[1 - \left(\frac{I}{\sigma_u}\right)\right]} \quad (\text{A.2.14})$$

Introducing the notation

$$S_e = \frac{4\sigma_u(b-1)}{(1-2\nu)\left[1-\left(\frac{\sigma_I}{\sigma_u}\right)\right]} \cong \frac{4\sigma_u(b-1)}{(1-2\nu)} \quad (\text{A.2.15})$$

we obtain

$$\frac{\pi d^2}{4} n_i = a_1 \frac{S_e}{p} \quad (\text{A.2.16})$$

Comparison of equations (A.2.9) and (A.2.16) shows that

$$S_e = 2S \quad (\text{A.2.17})$$

Accordingly equation (A.2.11) becomes

$$\frac{\pi d^2}{4} n_i = 3.7 \times 10^{-4} \left(\frac{S_e}{2P}\right)^{5.7} = 7.1 \times 10^{-6} \left(\frac{S_e}{P}\right)^{5.7} \quad (\text{A.2.18})$$

Thus in terms of  $S_e$  the incubation period is

$$\frac{\pi d^2}{4} n_i = 7.1 \times 10^{-6} \left(\frac{S_e}{P}\right)^{5.7} \quad (\text{A.2.19})$$

## REFERENCES

- [1] Lapp, R.R., Stutzman, R.H., Wahl, N.E., "A Study of the Rain Erosion of Plastic and Metals," WADC Technical Report 53-185, Part 2. Wright-Patterson Air Force Base, Dayton, Ohio. May 1955.
- [2] Lapp, R.R., Stutzman, R.H., Wahl, N.E., "Summary Report on the Rain Erosion of Aircraft Material," WADC Technical Report 53-185, Part 3. Wright-Patterson Air Force Base, Dayton, Ohio. Sept. 1956.
- [3] Lapp, R.R., Thorpe, D.H., Stutzman, R.H., Wahl, N.E., "The Study of Erosion of Aircraft Materials at High Speed in Rain," WADC Technical Report 53-185, Part 4. Wright-Patterson Air Force Base, Dayton, Ohio. May 1958.
- [4] Schmitt, G.F., Tatnall, G.J., Foulke, K.W., "Joint Air Force-Navy Supersonic Rain Erosion Evaluations of Materials," AFML TR-67-164. Air Force Materials Laboratory, Wright-Patterson Air Force Base, Dayton, Ohio. 1967.
- [5] Schmitt, G.F., "Research for Improved Subsonic and Supersonic Rain Erosion Resistant Material," AFML-TR-67-211, Air Force Materials Laboratory, Wright-Patterson Air Force Base, Dayton, Ohio. January 1968.
- [6] Schmitt, G.F., "Erosion Behavior of Polymeric Coatings and Composites at Subsonic Velocities," Proceedings of the Third International Conference on Rain Erosion and Associated Phenomena," (Edited by A.A. Fyall and R.B. King). Royal Aircraft Establishment, England. pp. 107-128. August, 1970.
- [7] Morris, J.W., "Supersonic Rain and Sand Erosion Research," AFML-TR-69-287, Part II. "Mechanic Investigation of Rain Erosion," Air Force Materials Laboratory, Wright-Patterson Air Force Base, Dayton, Ohio. September 1969.
- [8] Engel, O.G., A.J. Piekutowski, "Investigation of Composite-Coating Systems for Rain-Erosion Protection," Prepared under contract N00019-71-C-0108 for Naval Air Systems Command, Department of the Navy, at the University of Dayton, Research Institute, Dayton, Ohio.
- [9] Conn, A.F., "Research of Dynamic Response and Adhesive Failures of Rain Erosion Resistant Coating," Technical Report 811-1 Hydro-nautics, Laurel, MD. January 1969.
- [10] Conn, A.F., "Prediction of Rain Erosion Resistance from Measurements of Dynamic Properties," Technical Paper, Hydronautics, Laurel, MD. April 1970.
- [11] Conn, A.F., Rudy, S.L., "Further Research on Predicting the Rain Erosion Resistance of Material," Technical Report 7107-1, Hydronautics, Laurel, MD. May 1972.

- [12] Mok, C.H., "A Cumulative Damage Concept in Rain Erosion Studies," AIAA Journal, Vol. 7, pp. 751-753, 1969.
- [13] Springer, G.S., Baxi, C.B., "A Model for Rain Erosion of Homogeneous Material," Technical Report AFML-TR-72-106, Air Force Materials Laboratory, Wright-Patterson Air Force Base, Dayton, Ohio. June 1972.
- [14] Heymann, F.J., "Erosion by Cavitation, Liquid Impingement and Solid Impingement: A Review," Engineering Report E-1460, Westinghouse Electric Corporation, Lester, Pennsylvania, March 1968.
- [15] Heymann, F.J., "On the Shock Wave Velocity and Impact Pressure in High Speed Liquid-Solid Impact," Trans. ASME, J. of Basic Engineering, Vol. 90, pp. 400-405, 1968.
- [16] Brunton, J.H., "Liquid Impact and Material Removal Phenomena," Technical Memorandum No. 33-354, Jet Propulsion Laboratory, California Institute of Technology, Pasadena, California, June 1964.
- [17] Heymann, F.J., "A Survey of Clues to the Relation Between Erosion Rate and Impingement Conditions," Proceedings of the Second Meersburg Conference on Rain Erosion and Allied Phenomena, (Edited by A.A. Fyall and R.B. King), Royal Aircraft Establishment, Farnborough, England, pp. 683-760. August 1967.
- [18] Leith, W.C., Thompson, A.L., "Some Corrosion Effects in Accelerated Cavitation Damage," Trans. ASME, J. of Basic Engineering, Vol. 82D, pp. 795-807, 1960.
- [19] Mathieson, R., Hobbs, J.M., "Cavitation Erosion: Comparative Tests," Engineering, Vol. 189, pp. 136-137, 1960.
- [20] Ripken, J.F., "A Testing Rig for Studying Impingement and Cavitation Damage," in Erosion by Cavitation on Impingement, ASTM STP 408, American Society for Testing and Materials, pp. 3-11, 1967.
- [21] Thiruvengadam, A., Rudy, S.L., and Gunasekaran, M., "Experimental and Analytical Investigations on Liquid Impact Erosion," in Characterization and Determination of Erosion Resistance, ASTM STP 474, American Society for Testing and Materials, pp. 249-287, 1970.
- [22] Miner, M.A., "Cumulative Damage in Fatigue," J. Appl. Mech., Vol. 12, pp. A159-A164, 1945.
- [23] Timoshenko, S., Theory of Elasticity, McGraw-Hill Book Co., New York, 1934.
- [24] Juvinall, R.C., Stress, Strain and Strength, McGraw-Hill Book Co., New York, 1967.
- [25] Weibull, W., Fatigue Testing and Analysis of Results, Pergamon Press, New York, 1961.

- [26] Conn, A.F., "Discussion on 'Erosion Behavior of Polymeric Coating and Composites at Subsonic Velocity' by G.F. Schmitt," Proceedings of the Third International Conference on Rain Erosion and Associated Phenomena, (Edited by A.A. Fyall and R.B. King) Royal Aircraft Establishment, England, pp. 135-138. August 1970.
- [27] Morris, J.W., "Discussion on 'Erosion Behavior of Polymeric Coatings and Composites at Subsonic Velocity' by G.F. Schmitt," Proceedings of the Third International Conference on Rain Erosion and Associated Phenomena, (Edited by A.A. Fyall and R.B. King), Royal Aircraft Establishment, England. pp. 139-144.

Security Classification

## DOCUMENT CONTROL DATA - R &amp; D

*(Security classification of title, body of abstract and indexing annotation must be entered when the overall report is classified)*

1. ORIGINATING ACTIVITY (Corporate author) The University of Michigan Mechanical Engineering Department Ann Arbor, Michigan 48104		2a. REPORT SECURITY CLASSIFICATION UNCLASSIFIED	
		2b. GROUP	
3. REPORT TITLE "Analysis of Rain Erosion of Coated Materials"			
4. DESCRIPTIVE NOTES (Type of report and inclusive dates) Technical Report, June 1972-June 1973			
5. AUTHOR(S) (First name, middle initial, last name) George S. Springer Cheng-I. Yang Poul S. Larsen			
6. REPORT DATE September 1973	7a. TOTAL NO. OF PAGES 59	7b. NO. OF REFS 27	
8a. CONTRACT OR GRANT NO. F33615-72-C-1563	9a. ORIGINATOR'S REPORT NUMBER(S)		
b. PROJECT NO.			
c. Task No. 734007	9b. OTHER REPORT NO(S) (Any other numbers that may be assigned this report) AFML-TR-73-227		
d.			
10. DISTRIBUTION STATEMENT Approved for public release; distribution unlimited.			
11. SUPPLEMENTARY NOTES		12. SPONSORING MILITARY ACTIVITY Air Force Materials Laboratory Wright-Patterson Air Force Base Ohio 45433	
13. ABSTRACT <p>The behavior of coat-substrate systems subjected to repeated impingements of liquid droplets was investigated. The systems studied consisted of a thick homogeneous substrate covered by a single layer of homogeneous coating of arbitrary thickness. Based on the uniaxial stress wave model, the variations of the stresses with time were determined both in the coating and in the substrate. Employing the fatigue theorems established for the rain erosion of homogeneous materials, algebraic equations were derived which describe the incubation period, and the mass loss of the coating past the incubation period, in terms of the properties of the droplet, the coating and the substrate. The results were compared to available experimental data and good agreement was found between the present analytical results and the data.</p> <p>The differences between the uniaxial stress wave and the uniaxial strain wave models were also evaluated by calculating according to both models a) the stress at the coat-liquid interface, b) the stress that would occur in the substrate in the absence of the coating, and c) the stress in the coating after the first wave reflection from the substrate.</p>			

14.

KEY WORDS

LINK A

LINK B

LINK C

ROLE

WT

ROLE

WT

ROLE

WT

Rain Erosion  
Erosion Mechanism  
Fatigue Model  
Incubation Period

UNIVERSITY OF MICHIGAN



**3 9015 03526 6892**